Effect of vertex corrections on the charge and spin responses of the Fermi liquid

1996 J. Phys.: Condens. Matter 8 10435

(http://iopscience.iop.org/0953-8984/8/49/032)

J. Phys.: Condens. Matter **8** (1996) 10435–10455. Printed in the UK

Effect of vertex corrections on the charge and spin responses of the Fermi liquid

Y M Malozovsky and J D Fan

Department of Physics, Southern University and A & M College, Baton Rouge, LA 70813, USA

Received 13 May 1996, in final form 30 July 1996

Abstract. The effects of vertex corrections on the charge and spin responses of the Fermi liquid are considered. It is shown that the interaction in the particle–hole channel induces virtual pair excitations (Cooper pair like) in both the charge and the spin channels. It leads to the appearance of an anomalous Fermi-liquid term $\mathrm{Im}\,\tilde{\chi} \sim -\omega/T$ in both the charge and the spin responses of the Fermi liquid in addition to the normal response $\sim -\omega/v_F k$. Such a contribution of the anomalous term to the charge and spin responses is in agreement with the marginal Fermi-liquid hypothesis proposed by Varma *et al* to explain the universal anomalies in the normal state of cuprate high-T_c superconductors.

1. Introduction

The normal state of the high-temperature layered two-dimensional (2D) Cu–O oxides (cuprates) exhibits a number of unusual properties. Among them are the linear T-dependence of resistivity $\rho(T)$ [1–3], the inverse Hall coefficient $R_H^{-1}(T)$ [4, 5], the deviation of the optical conductivity $\sigma(\omega)$ [6] from the Drude theory, a flat electronic background in the Raman scattering intensity $S(\omega)$ [7, 8] and an anomalous T-dependence of the nuclear relaxation rate $T_1^{-1}(T)$ [9]. These features indicate that cuprates may radically differ from conventional metals. In an attempt to find the unified feature in the observed anomalies in the normal state of cuprates a hypothetical form of polarizability was proposed by Varma and co-workers [10–13]. It was stated that over a wide range of momenta $q(\omega < v_F q)$ in the system there exist excitations as follows which contribute to both the charge and the spin polarizabilities:

$$\mathrm{Im}\,[\tilde{\chi}(\boldsymbol{q}, \omega, T)] \propto \begin{cases} -N(0)\omega/T & \omega \ll T \\ -N(0) & T \ll \omega < \omega_c \end{cases} \tag{1}$$

where $N(0)$ is the unrenormalized single-particle density of states, and ω_c is the cut-off energy for a bosonic spectrum which is flat over a large frequency range $T < \omega < \omega_c$. This state with the spectrum of excitations in the form of equation (1) is termed the 'marginal' Fermi-liquid (MFL). In addition, it was pointed out [10, 11] that $\tilde{\chi}$ in equation (1) denotes the leading frequency contribution of the renormalized particle–hole excitations with the complete vertex, whereas the other term in the irreducible response is the leading frequency contribution of the particle–hole excitations without any vertex correction. Namely, the latter represents the conventional Fermi-liquid behaviour $\mathrm{Im}[\tilde{\chi}(\boldsymbol{q}, \omega)] \sim -N(0)\omega/v_F q$. The form of equation (1) implies that there exist in the Fermi system either non-degenerate current carriers with spin or excitations of some kind with the bosonic nature in the particle–hole

0953-8984/96/4910435+21$19.50

channel which make a contribution of the form of equation (1) to both the charge and the spin responses.

It is well known that the fluctuation pairing can make a significant contribution to the conductivity, magnetic susceptibility, specific heat, etc, of a superconducting metal in the normal state [14–16]. Moreover, even in the normal metal where the repulsion dominates in the interaction of electrons, a fluctuation pairing of electrons does occur. As a result, the fluctuation-induced paramagnetic susceptibility logarithmically depends on temperature in this case. This was first shown by Aslamazov and Larkin [14]. Effects due to the virtual pairing are especially significant in layered metals. In a layered 2D cuprate the Coulomb interaction is strong. In this case, virtual pairs (Cooper pair like) which appear in the particle–hole channel due to such a strong interaction and behave as Bose-like excitations can significantly modify the charge and spin responses of the Fermi liquid.

In this paper we shall show that the interaction in the particle–hole channel induces correlations in the 'Cooper' channel. Such correlations bring about the large vertex corrections in both the charge and the spin channels that lead the imaginary part of polarizability to the form of equation (1) in addition to the normal Fermi-liquid polarizability term $\sim -\omega/v_F k$. In other words, we shall show that in the particle–hole channel there exist virtual pair excitations (Cooper pair-like excitations) that make a contribution to both the charge and the spin responses of the Fermi liquid.

2. General relations and response in the charge channel

The goal of the paper is to get analytical expressions for the irreducible density response functions $\tilde{\chi}_c(\boldsymbol{k}, \omega)$ and $\tilde{\chi}_s(\boldsymbol{k}, \omega)$ in the charge and spin channels, respectively, incorporating the three-point vertex correction. The equation for the spin-dependent irreducible polarizability including the vertex function can be represented in the form [17–20]

$$\tilde{\chi}_{\sigma\sigma'}(k) = -\mathrm{i}\int \frac{\mathrm{d}^4 p'}{(2\pi)^4} G_\sigma(p')\Gamma_{\sigma\sigma'}(p', k)G_{\sigma'}(p' - k) \tag{2}$$

where p and k are the four-dimensional vectors, σ is the spin index, $G_\sigma(k)$ is the dressed electron Green function and $\Gamma_{\sigma\sigma'}(p', k)$ is the exact scalar three-point vertex function. The equation for the vertex function in the ladder approximation can be written as [17–20]

$$\Gamma_{\sigma\sigma'}(p', k) = \delta_{\sigma\sigma'} + \mathrm{i}\sum_{\sigma''}\int \frac{\mathrm{d}^4 p'}{(2\pi)^4} K^{\sigma\sigma''}(p, p')G_{\sigma''}(p')\Gamma_{\sigma''\sigma'}(p', k)G_{\sigma'}(p' - k) \tag{3}$$

where $K^{\sigma\sigma'}(p, p')$ denotes the kernel of the integral equation for the vertex function. It depends on the spin indices and describes the many-particle correlations. The diagrams for the irreducible polarizability, equation (2), and the equation for the vertex function, equation (3) are given in figure 1. The kernel $K^{\sigma\sigma'}(p, p')$ of the interaction in equation (3) satisfies Ward's identity [17–21] and can therefore be written as a functional derivative of the self-energy with respect to the electron Green function: $K^{\sigma\sigma'}(p, p') = -\mathrm{i}\,\delta\Sigma_\sigma(p)/\delta G_{\sigma'}(p')$, where we introduce the spin-dependent self-energy. The single-particle self-energy incorporating the vertex correction can thus be represented by [17–20]

$$\Sigma_\sigma(p) = \mathrm{i}\sum_{\sigma'}\int \frac{\mathrm{d}^4 k}{(2\pi)^4} G_{\sigma'}(p - k)D(k)\Gamma_{\sigma'\sigma}(p, k) \tag{4}$$

where $D(k)$ is the boson Green function. The boson Green function satisfies the Dyson equation $D(k) = D_0(k) + D_0(k)\tilde{\chi}(k)D(k)$, where $D_0(k)$ is the zeroth-order boson Green function and $\tilde{\chi}(k)$ is the irreducible response function in the charge-density channel. As an

example, in the case of the Coulomb interaction, $D_0(k) = V(\boldsymbol{k})$. From the Dyson equation follows the equation for the dielectric response function: $\varepsilon(k) = 1 - V(\boldsymbol{k})\tilde{\chi}(k)$. In the case of the electron–phonon interaction, $D_0(k) = D_{0ph}(\boldsymbol{k}, \omega) = 2g_0^2(\boldsymbol{k})\omega_0(\boldsymbol{k})/(\omega^2 - \omega_0^2(\boldsymbol{k}) + \mathrm{i}\delta)$, where $g_0(\boldsymbol{k})$ and $\omega_0(\boldsymbol{k})$ are the unrenormalized ('original') matrix element of the electron–phonon interaction and phonon frequency, respectively.

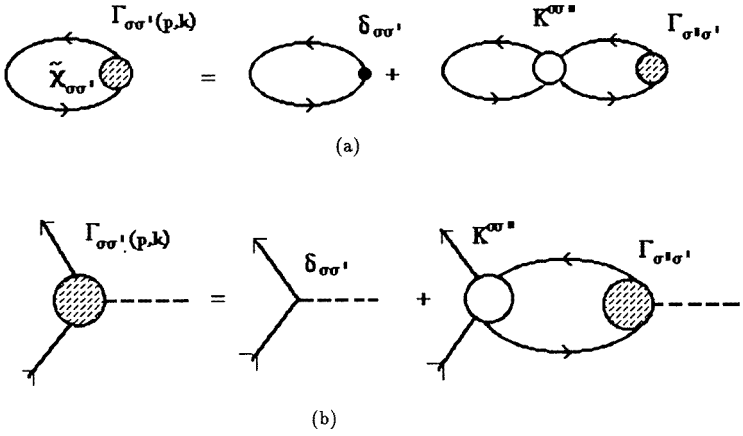

Figure 1. Diagrams for (a) the spin-dependent irreducible polarizability $\tilde{\chi}_{\sigma\sigma'}(k)$ and (b) the vertex function $\Gamma_{\sigma\sigma'}(p, k)$.

Now consider the kernel of interaction in the equation for the vertex part. To evaluate this kernel we use the iteration procedure and take the self-energy equation in the random-phase approximation (RPA) as a first approximation, i.e. equation (4) with $\Gamma_{\sigma\sigma'}(p, k) = \delta_{\sigma\sigma'}$ and $\tilde{\chi}(k) = \chi_0(k)$, where

$$\chi_0(k) = -\mathrm{i}\sum_{\sigma}\int \frac{\mathrm{d}^4 q}{(2\pi)^4} G_\sigma(q) G_\sigma(q - k)$$

is the free-particle response function. Using the relation $\delta G_\sigma(p)/\delta G_{\sigma'}(p') = \delta(p - p')\delta_{\sigma\sigma'}$, the expression for the kernel in the RPA can thus be derived as

$$K^{\sigma\sigma'}(p, p') = K_1^{\sigma\sigma'}(p, p') + K_2^{\sigma\sigma'}(p, p') \tag{5a}$$

where

$$K_1^{\sigma\sigma'}(p, p') = D(p - p')\delta_{\sigma\sigma'} \tag{5b}$$

and

$$K_2^{\sigma\sigma'}(p, p') = -\mathrm{i}\int \frac{\mathrm{d}^4 q}{(2\pi)^4} D^2(p - q) G_\sigma(q)[G_{\sigma'}(p' - p + q) + G_{\sigma'}(p' + p - q)] \tag{5c}$$

with the boson propagator $D(k)$ in the RPA. If a bisection of any electron line is used to represent δG_σ, the resulting diagram due to the cutting and stretching then represents $\delta\Sigma_\sigma/\delta G_{\sigma'}$. It is seen that the cutting at a, b and c of the top diagram of self-energy in figure 2 yields the three diagrams in figures 2(a), 2(b) and 2(c), respectively. Figure 2(a) corresponds to the first-order screened exchange interaction, whereas figures 2(b) and 2(c) correspond to the interactions in the particle–hole channel. Figure 2(b) corresponds to the second-order screened direct interaction. Figure 2(c) in the particle–hole channel is very important because it represents the interaction in the 'Cooper' channel (this diagram in fact

differs from the Cooper diagram since it has an opposite sign from the Cooper diagram and its initial and final momenta in scattering are the same). In analogy to the Cooper diagram, it has a logarithmic singularity [17] $\sim \ln(\omega_c/\max\{\omega, T\})$ if $\boldsymbol{p}' = -\boldsymbol{p}$ and $|\boldsymbol{p}| \approx p_F$, where ω_c is the characteristic cut-off frequency of the interaction $D(k)$ and p_F is the Fermi momentum. Further, it is necessary to distinguish between the interactions in the charge-density channel from those in the spin-density channel. For this purpose we can introduce the spin-symmetric and spin-asymmetric expressions for the interactions taking into account the property $K^{\sigma\sigma'}(p, p') = K^{-\sigma-\sigma'}(p, p')$ (which is valid in the paramagnetic phase $G_\uparrow(p) = G_\downarrow(p) = G(p)$). Thus, the spin-symmetric and spin-asymmetric interactions take the forms

$$K_c(p, p') = K^{\uparrow\uparrow}(p, p') + K^{\uparrow\downarrow}(p, p') = K_1(p, p') + 2K_2(p, p') \tag{6a}$$

and

$$K_c(p, p') = K^{\uparrow\uparrow}(p, p') + K^{\uparrow\downarrow}(p, p') = K_1(p, p') = D(p - p') \tag{6b}$$

where $K_c(p, p')$ and $K_s(p, p')$ are the kernels of interaction in the charge and spin channels, respectively.

The same relations can be written for the vertex and irreducible response functions. For instance, using equation (6) in equation (3) we have $\Gamma_{c,s}(p, k) = \Gamma_{\uparrow\uparrow}(p, k) \pm \Gamma_{\uparrow\downarrow}(p, k)$. The vertex functions in the charge and spin channels, respectively, are determined from the solution of these equations:

$$\Gamma_{c,s}(p, k) = 1 + \mathrm{i}\int \frac{\mathrm{d}^4 p'}{(2\pi)^4} K_{c,s}(p, p')G(p')G(p' - k)\Gamma_{c,s}(p' - k) \tag{7}$$

where $K_{c,s}(p, p')$ are given by equation (6). Thus, using equation (6*a*) in equation (7), one obtains the equation for $\Gamma_c(p, k)$, the vertex part in the charge channel. This is shown diagramatically in figure 3(a). Moreover, using equation (6*b*) in equation (7), one has the equation for $\Gamma_s(p, k)$, the vertex part in the spin channel (figure 3(b)). In terms of the relations for $\Gamma_{c,s}(p, k)$ and equation (2), the irreducible response functions in the charge and spin channels can be written as

$$\tilde{\chi}_{c,s}(k) = 2[\tilde{\chi}_{\uparrow\uparrow}(k) \pm \tilde{\chi}_{\uparrow\downarrow}(k)] = -2\mathrm{i}\int \frac{\mathrm{d}^4 p'}{(2\pi)^4} G(p')G(p' - k)\Gamma_{c,s}(p', k). \tag{8}$$

Diagrams for $\tilde{\chi}_c(k)$ and $\tilde{\chi}_s(k)$ are shown in figure 3.

In addition, it can be shown [22] that the kernel $K^{\sigma\sigma'}(p, p')$ of the interaction in equation (3) is related to the Landau Fermi-liquid interaction function $f^{\sigma\sigma'}(\boldsymbol{p}, \boldsymbol{p}')$ in the form $K^{\sigma\sigma'}(\boldsymbol{p}, \xi_{\boldsymbol{p}}; \boldsymbol{p}', \xi_{\boldsymbol{p}'}) = -Z^{-1}(0) f^{\sigma\sigma'}(\boldsymbol{p}, \boldsymbol{p}')$, where $Z^{-1}(0) = 1 - \partial\Sigma/\partial\omega\,|_{\omega=0, p=p_F}$ is the renormalization parameter, and $\xi_{\boldsymbol{p}}$ is the quasi-particle energy measured relative to the Fermi energy. The result for $f^{\sigma\sigma'}(\boldsymbol{p}, \boldsymbol{p}')$ using equations (5*a*)–(5*c*) coincides with Rice's result [23] if we assume that $Z(0) = 1$. The relation between $K^{\sigma\sigma'}(p, p')$ and $f^{\sigma\sigma'}(\boldsymbol{p}, \boldsymbol{p}')$ will allow us to compare further the results in this paper with the phenomenology of the Landau Fermi liquid.

Further, the interactions in equation (6) are frequency and momentum dependent in a complicated way. For example, in the case of the Coulomb interaction, $D_0(k) = V(\boldsymbol{k})$, the frequency dependence of interactions covers both the high-frequency region (the plasma excitations) and the low-frequency region (the particle–hole excitations). In the case of the electron–phonon interaction the phonon Green function $D(\boldsymbol{k}, \omega)$ has cut-offs for the momentum $k_c \approx k_D$ and for the frequency $\omega_c \approx \omega_D$. In this paper we assume that the electron–boson interaction has the momentum and frequency extents of the order of the Fermi energy, i.e. $k_c \approx 2p_F$ and $\omega_c \approx \varepsilon_F$. This assumption allows us to concentrate our

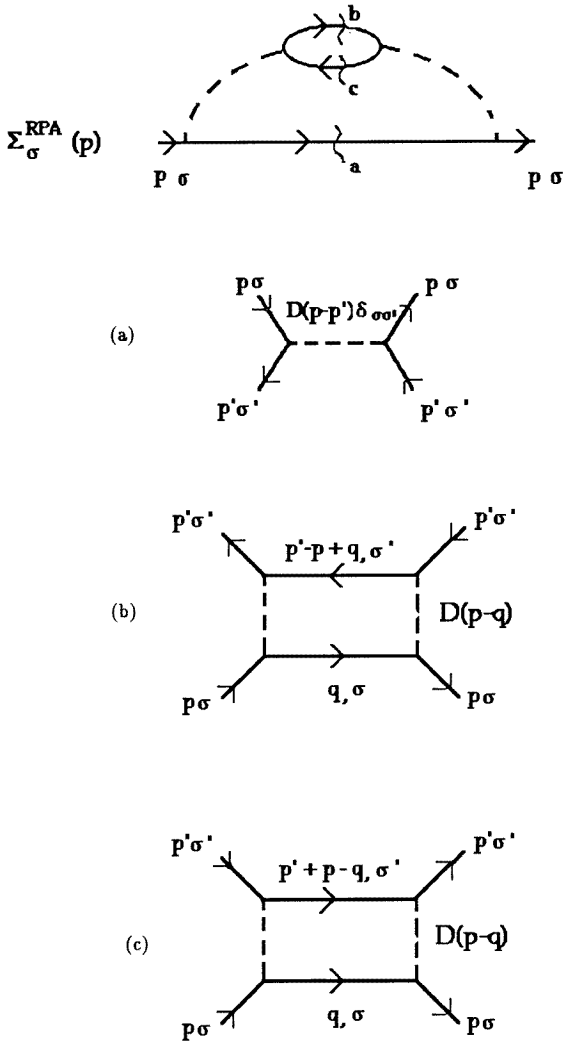

Figure 2. The graphical functional derivative of the RPA diagram for the self-energy with respect to the electron Green function. The resulting diagram due to the cutting of any electron line and stretching corresponds to the functional derivative of the self-energy, $\delta\Sigma_\sigma(p)/\delta G_{\sigma'}(p')$, i.e. the kernel of interaction. (a) The screened exchange interaction of the first order: (b) The direct interaction of the second order: (c) The 'Cooper' diagram. The broken lines correspond to the boson Green function in the RPA.

attention only on the particle–hole excitations in order to describe the vertex corrections in an electron liquid, and to take a frequency-independent interaction in the RPA for $\omega < v_F k$, i.e. $D(\boldsymbol{k}, \omega) \approx D(\boldsymbol{k}, 0) = D(\boldsymbol{k})$ in equation (6) as can be proved. Thus, our consideration is, in fact, more suitable for the non-retarded interaction like the pure Coulomb interaction when $D_0(k) = V(\boldsymbol{k})$. Indeed, in this case, $D(\boldsymbol{k}, \omega) = V(\boldsymbol{k})/[1 - V(\boldsymbol{k})\chi_0(\boldsymbol{k}, \omega)]$ with $\chi_0(\boldsymbol{k}, \omega) \approx \chi_0(\boldsymbol{k}, 0) \approx -N_F$ for $\omega < v_F k$ (e.g. in the isotropic 2D case $\chi_0(\boldsymbol{k}, \omega) \approx \chi_0(\boldsymbol{k}, 0) = -N_F[1 - \mathrm{Re}\sqrt{1 - 4p_F^2/k^2}]$, for $\omega < v_F k$, where $N_F = m^*/\pi$ is the 2D density

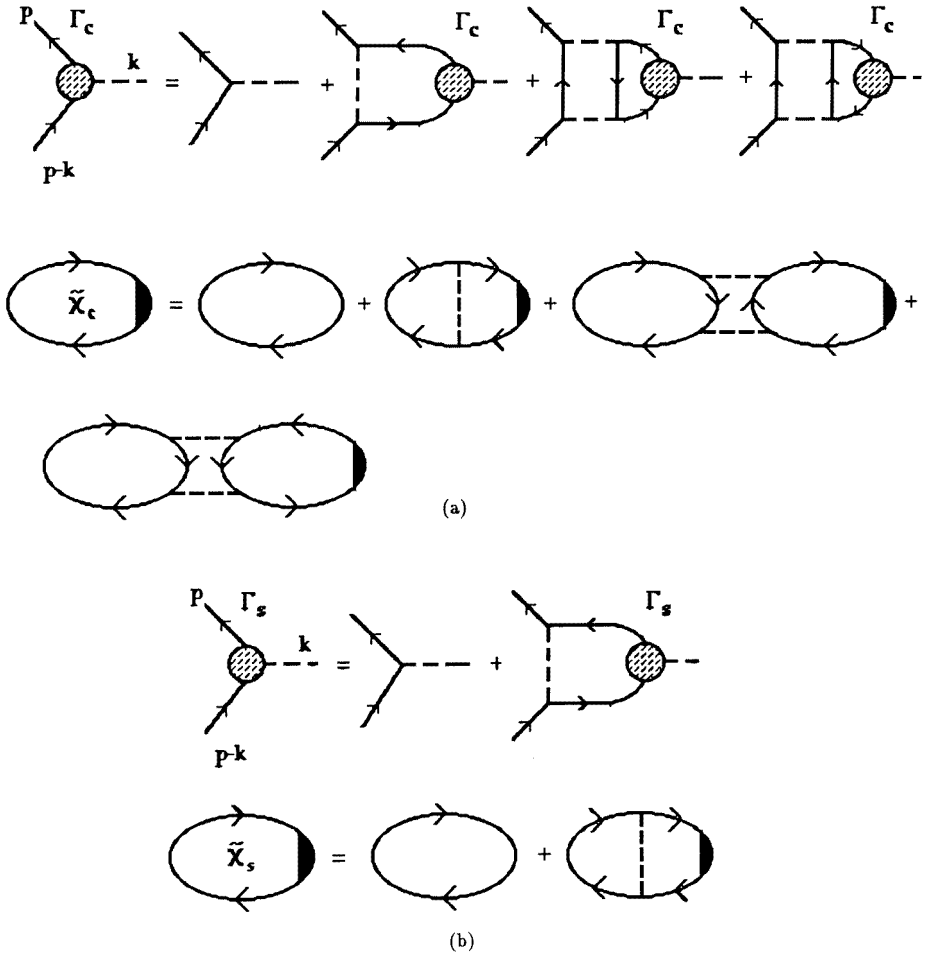

Figure 3. Diagram representation of equations for (a) $\Gamma_c(p,k)$ and $\tilde{\chi}_c(k)$ and (b) $\Gamma_s(p,k)$ and $\tilde{\chi}_s(k)$. The broken lines represent the boson Green function in the RPA as in figure 2.

of states, whereas $\mathrm{Im}[\chi_0(\boldsymbol{k},\omega)] \approx -N_F\omega/v_Fk \gg -N_F$ in this case). It is also understood that, in the case of the frequency-independent interaction $D(k)$, the well known Migdal [18] theorem is violated and the vertex corrections should be included in all the orders of perturbation theory.

Let us evaluate the response in the charge-density channel and, therefore, consider equation (6*a*). Noting that $D(k)$ is frequency independent in the particle–hole channel, and that the electron Green function is given by $G^{-1}(\boldsymbol{k},\mathrm{i}\omega) = \mathrm{i}\omega - \xi_{\boldsymbol{k}}$, where $\xi_{\boldsymbol{k}} = \varepsilon_{\boldsymbol{k}} - \mu$ is the single-particle energy $\varepsilon_{\boldsymbol{k}}$ measured relative to the chemical potential μ. Carrying out the frequency summation [17, 21], equation (6*a*) turns into the form

$$K_c(\boldsymbol{p},\mathrm{i}\omega;\boldsymbol{p}',\mathrm{i}\omega') = D(\boldsymbol{p}-\boldsymbol{p}') + 2\sum_{\boldsymbol{q}} D^2(\boldsymbol{p}-\boldsymbol{q})\frac{n_F(\xi_{\boldsymbol{q}}) - n_F(\xi_{\boldsymbol{q}-\boldsymbol{p}+\boldsymbol{p}'})}{\xi_{\boldsymbol{q}} - \xi_{\boldsymbol{q}-\boldsymbol{p}+\boldsymbol{p}'} - \mathrm{i}(\omega-\omega')}$$
$$-2\sum_{\boldsymbol{q}} D^2(\boldsymbol{p}-\boldsymbol{q})\frac{1 - n_F(\xi_{\boldsymbol{q}}) - n_F(\xi_{\boldsymbol{p}'+\boldsymbol{p}-\boldsymbol{q}})}{\mathrm{i}(\omega+\omega') - \xi_{\boldsymbol{q}} - \xi_{\boldsymbol{p}'+\boldsymbol{p}-\boldsymbol{q}}}. \tag{9}$$

Actually, the second term in equation (9) in the particle–hole channel is almost frequency independent. The last term in equation (9) is invariant under the transformation $\boldsymbol{p}'+\boldsymbol{p}-\boldsymbol{q}=\boldsymbol{Q}$ and $\boldsymbol{Q}\rightarrow\boldsymbol{q}$. This also follows from figure 2(c), i.e. the 'Cooper' diagram. Thus, changing the variables in the numerator, it can be written that

$$K_c^{pair}(\boldsymbol{p},\mathrm{i}\omega;\boldsymbol{p}',\mathrm{i}\omega')=-2\sum_{\boldsymbol{q}}D^2(\boldsymbol{p}-\boldsymbol{q})\frac{1-2n_F(\xi_{\boldsymbol{q}})}{\mathrm{i}(\omega+\omega')-\xi_{\boldsymbol{q}}-\xi_{\boldsymbol{p}+\boldsymbol{p}'-\boldsymbol{q}}}.$$

Therefore, it follows from equation (9) that the frequency dependence of the kernel is mainly due to the last term. The real part of it has the logarithmic singularity $\mathrm{Re}[K_c^{pair}(\boldsymbol{p},\omega;-\boldsymbol{p},\omega)]\sim\ln(\varepsilon_F/\max\{\omega,T\})$ for $\boldsymbol{p}'=-\boldsymbol{p}$ and $|\boldsymbol{p}|\approx p_F$, similar to the Cooper problem, where $\mu=\varepsilon_F$ (the Fermi energy) was assumed, while the imaginary part $\mathrm{Im}[K_c^{pair}(\boldsymbol{p},\omega;-\boldsymbol{p},\omega)\sim\tanh(\omega/2T)$ in this case. Using equation (9), taking $\Gamma_c(p',k)=1$ for the integrand in equation (7), and carrying out the frequency summation, we can find the vertex correction of the first order in the charge-density channel as follows:

$$\Gamma_c^{(1)}(\boldsymbol{p},\mathrm{i}\omega;\boldsymbol{k},\mathrm{i}\omega')=1+\Delta\Gamma_c^{(1)}(\boldsymbol{p},\mathrm{i}\omega;\boldsymbol{k},\mathrm{i}\omega') \tag{10}$$

where

$$\Delta\Gamma_c^{(1)}(\boldsymbol{p},\mathrm{i}\omega;\boldsymbol{k},\mathrm{i}\omega')=-\sum_{\boldsymbol{p}'}\left(\frac{n_F(\xi_{\boldsymbol{p}'})}{\xi_{\boldsymbol{p}'}-\xi_{\boldsymbol{p}'-\boldsymbol{k}}-\mathrm{i}\omega'}K_c(\boldsymbol{p},\mathrm{i}\omega;\boldsymbol{p}',\xi_{\boldsymbol{p}'})\right.$$
$$\left.-\frac{n_F(\xi_{\boldsymbol{p}'-\boldsymbol{k}})}{\xi_{\boldsymbol{p}'}-\xi_{\boldsymbol{p}'-\boldsymbol{k}}-\mathrm{i}\omega'}K_c(\boldsymbol{p},\mathrm{i}\omega;\boldsymbol{p}',\xi_{\boldsymbol{p}'-\boldsymbol{k}}+\mathrm{i}\omega')\right) \tag{11}$$

and $n_F(\omega)=[\exp(\omega/T)+1]^{-1}$ is the Fermi distribution function. In the region of the particle–hole excitations ($|\omega'|\ll v_Fk$), equation (11) can be written as

$$\Delta\Gamma_c^{(1)}(\boldsymbol{p},\mathrm{i}\omega;\boldsymbol{k},\mathrm{i}\omega')=-\sum_{\boldsymbol{p}'}\chi^0_{\boldsymbol{p}'\boldsymbol{k}}(\omega')K_c(\boldsymbol{p},\mathrm{i}\omega;\boldsymbol{p}',\xi_{\boldsymbol{p}'-\boldsymbol{k}}+\mathrm{i}\omega') \tag{12}$$

where

$$\chi^0_{\boldsymbol{p}\boldsymbol{k}}(\omega)=[n_F(\xi_{\boldsymbol{p}})-n_F(\xi_{\boldsymbol{p}-\boldsymbol{k}})]/(\xi_{\boldsymbol{p}}-\xi_{\boldsymbol{p}-\boldsymbol{k}}-\mathrm{i}\omega). \tag{13}$$

It follows from equation (12) that the vertex correction is frequency dependent. Using equation (10) in equation (8), the irreducible charge-density response function including the first-order vertex correction can be represented by

$$\tilde{\chi}_c^{(1)}(\boldsymbol{k},\mathrm{i}\omega)=2\sum_{\boldsymbol{p}}\left(\frac{n_F(\xi_{\boldsymbol{p}})}{\xi_{\boldsymbol{p}}-\xi_{\boldsymbol{p}-\boldsymbol{k}}-\mathrm{i}\omega)}\Gamma_c^{(1)}(\boldsymbol{p},\xi_{\boldsymbol{p}};\boldsymbol{k},\mathrm{i}\omega)\right.$$
$$\left.-\frac{n_F(\xi_{\boldsymbol{p}-\boldsymbol{k}})}{\xi_{\boldsymbol{p}}-\xi_{\boldsymbol{p}-\boldsymbol{k}}-\mathrm{i}\omega}\Gamma_c^{(1)}(\boldsymbol{p},\xi_{\boldsymbol{p}-\boldsymbol{k}}+\mathrm{i}\omega;\boldsymbol{k},\mathrm{i}\omega)\right)$$
$$\approx 2\sum_{\boldsymbol{p}}\chi^0_{\boldsymbol{p}\boldsymbol{k}}(\omega)\Gamma_c^{(1)}(\boldsymbol{p},\xi_{\boldsymbol{p}-\boldsymbol{k}}+\mathrm{i}\omega;\boldsymbol{k},\mathrm{i}\omega) \tag{14}$$

where $\chi^0_{\boldsymbol{p}\boldsymbol{k}}(\omega)$ is given by equation (13). Equation (14) is valid in the region of the particle–hole excitations ($|\omega|\ll v_Fk$).

Now, using equations (10) and (12) in equation (14), we have

$$\tilde{\chi}_c^{(1)}(\boldsymbol{k},\mathrm{i}\omega)=\chi_0(\boldsymbol{k},\mathrm{i}\omega)-2\sum_{\boldsymbol{p},\boldsymbol{p}'}\chi^0_{\boldsymbol{p}\boldsymbol{k}}(\omega)\chi^0_{\boldsymbol{p}'\boldsymbol{k}}(\omega)K_c(\boldsymbol{p},\xi_{\boldsymbol{p}-\boldsymbol{k}}+\mathrm{i}\omega;\boldsymbol{p}',\xi_{\boldsymbol{p}'-\boldsymbol{k}}+\mathrm{i}\omega). \tag{15}$$

Furthermore, using equation (9) for $K_c(\boldsymbol{p},\mathrm{i}\omega;\boldsymbol{p},\mathrm{i}\omega')$ in equation (15), one can see that $\tilde{\chi}_c^{(1)}(\boldsymbol{k},\mathrm{i}\omega)$ has two different contributions: the first is the usual contribution of the single-particle (single-pair) excitations corrected by the vertex correction, and the second

corresponds to the contribution of the virtual pair excitations (Cooper pair-like excitations, corresponding to two excited quasi-particles and two excited quasi-holes coupled together) in the particle–hole channel ($\omega \ll v_F k$). The contribution of the virtual pair excitations to $\tilde{\chi}_c^{(1)}(\boldsymbol{k}, \mathrm{i}\omega)$ is given by the last term in equation (9) while the others in equation (9) make a contribution to $\mathrm{Re}[\Gamma_c^{(1)}(\boldsymbol{p}, \mathrm{i}\omega; \boldsymbol{k}, \mathrm{i}\omega')]$ only. Thus, using equation (9) in equation (15), $\tilde{\chi}_{c\,pair}^{(1)}(\boldsymbol{k}, \mathrm{i}\omega)$, which is the contribution of the virtual pair excitations to $\tilde{\chi}_c^{(1)}(\boldsymbol{k}, \mathrm{i}\omega)$, can be written as

$$\tilde{\chi}_{c\,pair}^{(1)}(\boldsymbol{k}, \mathrm{i}\omega) \approx 4\langle D^2\rangle \sum_{\substack{\boldsymbol{p},\boldsymbol{p}',\boldsymbol{q} \\ |\xi_q|\leqslant\varepsilon_F}} \chi_{\boldsymbol{pk}}^0(\omega)\chi_{\boldsymbol{p}'\boldsymbol{k}}^0(\omega)\frac{1-2n_F(\xi_q)}{2\mathrm{i}\omega+\xi_{\boldsymbol{p}-\boldsymbol{k}}+\xi_{\boldsymbol{p}'-\boldsymbol{k}}-\xi_{\boldsymbol{q}}-\xi_{\boldsymbol{p}'+\boldsymbol{p}-\boldsymbol{q}}} \tag{16}$$

where $\chi_{\boldsymbol{pk}}^0(\omega)$ is given by equation (13), and the angular average of $D(\boldsymbol{p}-\boldsymbol{q})$ between $\boldsymbol{p}$ and $\boldsymbol{q}$ was made. In addition, equation (16) diverges at large q. This is due to the approximation of the angular averaging for $D^2(\boldsymbol{q})$. Equation (15) does not have such a divergence because of the fast decay of $D^2(\boldsymbol{q})$ on increase in $q > 2p_F$. Therefore, the upper limit for q in equation (16) is approximately equal to $2p_F$. The diagram for $\tilde{\chi}_{c\,pair}^{(1)}(\boldsymbol{k}, \mathrm{i}\omega)$ is shown in the last diagram of figure 3(a) for $\tilde{\chi}_c(k)$. It can be shown that the major contribution of the last diagram in figure 3(a) comes from the state $\boldsymbol{p}' = -\boldsymbol{p}$. Therefore, in the summation over $\boldsymbol{p}$ and $\boldsymbol{p}'$ in equation (16), the major contribution comes from the pairing states $\{\boldsymbol{p}', \boldsymbol{p}\} = (-\boldsymbol{p}_1, \boldsymbol{p}_1), (-\boldsymbol{p}_2, \boldsymbol{p}_2), \ldots (-\boldsymbol{p}_n, \boldsymbol{p}_n)$. Thus, carrying out the summation over $\boldsymbol{p}$ and $\boldsymbol{p}'$ in equation (16), we can see that the coherent states (i.e. the pairing states with $\boldsymbol{p}' = -\boldsymbol{p}$ and $|\boldsymbol{p}| \approx p_F$) contribute only to $\mathrm{Im}[\tilde{\chi}_{c\,pair}^{(1)}(\boldsymbol{k}, \mathrm{i}\omega)]$ in the particle–hole channel ($|\omega| \ll v_F k$), whereas other states ($\boldsymbol{p}' \neq -\boldsymbol{p}$) give a small contribution of the order $\sim 1/\varepsilon_F$. In this case $\xi_{\boldsymbol{p}-\boldsymbol{k}} + \xi_{\boldsymbol{p}'-\boldsymbol{k}} \approx 0 (\ll 2|\omega|)$ because $\boldsymbol{p} = -\boldsymbol{p}'$ and $|\boldsymbol{p}| \approx p_F$. Thus, after the analytical continuation to the real axes ($\mathrm{i}\omega \to \omega + \mathrm{i}\delta$) the imaginary part of $\tilde{\chi}_{c\,pair}^{(1)}(\boldsymbol{k}, \mathrm{i}\omega)$ is given by

$$\begin{aligned}\mathrm{Im}[\tilde{\chi}_{c\,pair}^{(1)}(\boldsymbol{k}, \omega)_{|\omega\ll v_F k}] &= -\frac{\pi}{2}N_F^2\langle D^2\rangle \sum_{|\xi_q|\leqslant\varepsilon_F}^{\boldsymbol{q}} [1-2n_F(\xi_q)]\delta(\omega-\xi_q) \\ &= -\frac{\pi}{4}N_F^3\langle D^2\rangle \tanh\left(\frac{\omega}{2T}\right)\end{aligned} \tag{17}$$

where $\omega \leqslant \varepsilon_F$, and N_F is the quasi-particle density of states (in an isotropic 2D electron spectrum, $N_F = m^*/\pi$, where m^* is the effective mass). The real part of $\tilde{\chi}_{c\,pair}^{(1)}(\boldsymbol{k}, \mathrm{i}\omega)$ in the static ($\omega \approx 0$) and long-wavelength limit ($k \approx 0$) has the form

$$\mathrm{Re}[\tilde{\chi}_{c\,pair}^{(1)}(0,0)] = -\tfrac{1}{2}N_F\lambda^2 \ln\left(\frac{2\gamma_E\varepsilon_F}{\pi T}\right) = -N_F\lambda - \tfrac{1}{2}N_F\lambda^2\ln\left(\frac{T^*}{T}\right) \tag{17a}$$

where $\lambda^2 = N_F^2\langle D^2\rangle$ is the coupling constant, and $T^* = 1.13\varepsilon_F \exp(-2/\lambda)$ is the characteristic temperature. One can see from equation (17*a*) that, in the case of weak coupling ($\lambda \ll 1$), T^* is very low and the contribution of the virtual pairs to the real part of the charge response is also small (e.g., at $T = T^*$, $\mathrm{Re}[\tilde{\chi}_{c\,pair}^{(1)}(0,0)] \approx -N_F\lambda$, where $\mathrm{Re}[\chi_0(0,0)] \approx -N_F$), but this contribution becomes significant in the case of intermediate or strong coupling when $\lambda \approx 1$. Thus, equation (17*a*) exhibits the effect of the virtual pairs on the charge-density response. It appears in the second order in terms of λ with the logarithmic temperature dependence and is similar to the result obtained by Aslamazov and Larkin [14].

Finally, the imaginary part of $\tilde{\chi}_c^{(1)}(\boldsymbol{k}, \mathrm{i}\omega)$, the irreducible response function in the charge channel including the conventional Fermi-liquid response, using equations (9), (16) and (17),

can be written as

$$\mathrm{Im}[\tilde{\chi}_c^{(1)}(\boldsymbol{k},\omega)_{|\omega\ll v_F k}] \approx -N_F\left\{\frac{\omega}{v_F k}\,\mathrm{Re}[\Gamma_c^{(1)}(p_F,0;0,0)]+\frac{\pi}{4}N_F^2\langle D^2\rangle\tanh\left(\frac{\omega}{2T}\right)\right\} \tag{18}$$

It follows from equation (18) that in the weak-coupling limit ($\langle D\rangle N_F \ll 1$) the second term in the brackets is small in comparison with the first and $\mathrm{Im}[\tilde{\chi}_c^{(1)}(\boldsymbol{k},\omega)_{|\omega\ll v_F k}] \sim -N_F\omega/v_F k$ becomes the form of the standard Fermi-liquid result. However, in the case of intermediate and strong coupling ($\langle D\rangle N_F \leqslant 1$), it follows from equation (18) that $\mathrm{Im}[\tilde{\chi}_c^{(1)}(\boldsymbol{k},\omega)_{|\omega\ll v_F k}] \approx -N_F\lambda^2\tanh(\omega/2T)$, where $\lambda = \langle D\rangle N_F$ is the effective interelectron coupling constant in the charge channel as before. Thus, in the case when $\lambda \leqslant 1$, equation (18) is similar to equation (1) and hence follows the hypothesis of Varma *et al* [10].

Such an unusual behaviour of the irreducible response can be explained as follows. In the weak-coupling limit ($\lambda \ll 1$), only the single-particle excitations make a contribution to the response of the Fermi liquid because the contribution of the virtual pair excitations (two quasi-particles and two quasi-holes excited from the Fermi sea and coupled together) is weak. In the case when $\lambda \leqslant 1$, when correlations in the 'Cooper' channel become stronger, the virtual pair excitations—Cooper pair-like excitations—are more important and make a major contribution to the charge response of the Fermi liquid while the single-particle excitations in this case are less important. Moreover, Cooper pair-like excitations, similar to a non-degenerate gas, make a contribution $\sim -\omega/T$ to the charge response.

The form of the charge response in the strong-coupling limit (i.e. $\mathrm{Im}[\tilde{\chi}_c^{(1)}(\boldsymbol{k},\omega)_{|\omega\ll v_F k}] \sim -N_F\tanh(\omega/2T)$, where $\lambda \approx 1$ was assumed) is somehow similar to that of the nested Fermi liquid (NFL) proposed by Virosztek and Ruvalds [24] in an attempt to develop a microscopic basis for equation (1), the MFL model. The susceptibility for the nested fermions [24] in the form of $\mathrm{Im}[\tilde{\chi}_0^{NFL}(\boldsymbol{k}\approx\boldsymbol{Q},\omega)] \sim -N_F\tanh(\omega/4T)$ exists only for a particular momentum transfer $\boldsymbol{Q}$, the nesting wavevector, without including any vertex corrections, and the Fermi surface should have the ideal nesting features as well. Moreover, in the framework of the NFL the normal response is missing. Our approach, incorporating the vertex corrections, leads to the response which includes the normal response as well as the anomalous MFL response.

Further, using equations (10) and (11), we can find the equation for the vertex correction up to the second order (from equation (7)) as follows:

$$\begin{aligned}\Gamma_c^{(2)}(\boldsymbol{p},\mathrm{i}\omega;\boldsymbol{k},\mathrm{i}\omega') &= 1+\Delta\Gamma_c^{(1)}(\boldsymbol{p},\mathrm{i}\omega;\boldsymbol{k},\mathrm{i}\omega')\\ &\quad-\sum_{\boldsymbol{p}'}\left(\frac{n_F(\xi_{\boldsymbol{p}'})}{\xi_{\boldsymbol{p}'}-\xi_{\boldsymbol{p}'-\boldsymbol{k}}-\mathrm{i}\omega'}K_c(\boldsymbol{p},\mathrm{i}\omega;\boldsymbol{p}',\xi_{\boldsymbol{p}'})\,\Delta\Gamma_c^{(1)}(\boldsymbol{p}',\xi_{\boldsymbol{p}'};\boldsymbol{k},\mathrm{i}\omega')\right.\\ &\quad\left.-\frac{n_F(\xi_{\boldsymbol{p}'-\boldsymbol{k}})}{\xi_{\boldsymbol{p}'}-\xi_{\boldsymbol{p}'-\boldsymbol{k}}-\mathrm{i}\omega'}K_c(\boldsymbol{p},\mathrm{i}\omega;\boldsymbol{p}',\xi_{\boldsymbol{p}'-\boldsymbol{k}}+\mathrm{i}\omega')\,\Delta\Gamma_c^{(1)}(\boldsymbol{p}',\xi_{\boldsymbol{p}'-\boldsymbol{k}}+\mathrm{i}\omega';\boldsymbol{k},\mathrm{i}\omega')\right)\\ &\approx 1+\Delta\Gamma_c^{(1)}(\boldsymbol{p},\mathrm{i}\omega;\boldsymbol{k},\mathrm{i}\omega')\\ &\quad-\sum_{\boldsymbol{p}'}\tilde{\chi}^0_{\boldsymbol{p}'\boldsymbol{k}}(\omega')K_c(\boldsymbol{p},\mathrm{i}\omega;\boldsymbol{p}',\xi_{\boldsymbol{p}'-\boldsymbol{k}}+\mathrm{i}\omega')\,\Delta\Gamma_c^{(1)}(\boldsymbol{p}',\xi_{\boldsymbol{p}'-\boldsymbol{k}}+\mathrm{i}\omega';\boldsymbol{k},\mathrm{i}\omega')\end{aligned} \tag{19}$$

Noting that in the summation over $\boldsymbol{p}'$ in equation (19) the major contribution comes from $|\boldsymbol{p}'| \approx p_F$, we can therefore replace $\Delta\Gamma_c^{(1)}(\boldsymbol{p}',\xi_{\boldsymbol{p}'-\boldsymbol{k}}+\mathrm{i}\omega';\boldsymbol{k},\mathrm{i}\omega')$ in equation (19) by its average over the Fermi surface, i.e. $\Delta\Gamma_c^{(1)}(\boldsymbol{p}',\xi_{\boldsymbol{p}'-\boldsymbol{k}}+\mathrm{i}\omega';\boldsymbol{k},\mathrm{i}\omega')$ turns into $\langle\Delta\Gamma_c^{(1)}(\boldsymbol{p}',\xi_{\boldsymbol{p}'-\boldsymbol{k}}+\mathrm{i}\omega';\boldsymbol{k},\mathrm{i}\omega')\rangle_{|\boldsymbol{p}'|=p_F}$. Then equation (19) can approximately be written as

$$\Gamma_c^{(2)}(\boldsymbol{p},\mathrm{i}\omega;\boldsymbol{k},\mathrm{i}\omega') \approx 1+\Delta\Gamma_c^{(1)}(\boldsymbol{p},\mathrm{i}\omega;\boldsymbol{k},\mathrm{i}\omega')\langle\Gamma_c^{(1)}(\boldsymbol{p}',\xi_{\boldsymbol{p}'-\boldsymbol{k}}+\mathrm{i}\omega';\boldsymbol{k},\mathrm{i}\omega')\rangle_{|\boldsymbol{p}'|=p_F}. \tag{20}$$

Similarly, we can obtain the vertex correction up to the third order $\Gamma_c^{(3)}(p,k)$, and so on up to the nth order $\Gamma_c^{(n)}(p,k)$, and express them in terms of $\Delta\Gamma_c^{(1)}(p,k)$. It is obvious that the expression of $\Gamma_c^{(n)}(p,k)$, is a series of $\Delta\Gamma_c^{(1)}(p,k)$ and $\Gamma_c(p,k) = \lim_{n\to\infty}[\Gamma_c^{(n)}(p,k)]$. Making the necessary summation of the series ('ladder'), the vertex correction can be evaluated as

$$\Gamma_c(\boldsymbol{p}, \mathrm{i}\omega; \boldsymbol{k}, \mathrm{i}\omega') \approx 1 + \frac{\Delta\Gamma_c^{(1)}(\boldsymbol{p}, \mathrm{i}\omega; \boldsymbol{k}, \mathrm{i}\omega')}{1 - \langle\Delta\Gamma_c^{(1)}(\boldsymbol{p}, \xi_{\boldsymbol{p}-\boldsymbol{k}} + \mathrm{i}\omega'; \boldsymbol{k}, \mathrm{i}\omega')\rangle_{|\boldsymbol{p}|=p_F}}. \tag{21}$$

In the denominator of equation (21), $\langle\Delta\Gamma_c^{(1)}(\boldsymbol{p}, \xi_{\boldsymbol{p}-\boldsymbol{k}}+\mathrm{i}\omega'; \boldsymbol{k}, \mathrm{i}\omega')\rangle_{|\boldsymbol{p}|=p_F}$, using equations (9) and (12), can be represented by

$$\langle\Delta\Gamma_c^{(1)}(\boldsymbol{p}, \xi_{\boldsymbol{p}-\boldsymbol{k}} + \mathrm{i}\omega; \boldsymbol{k}, \mathrm{i}\omega)\rangle_{|\boldsymbol{p}|=p_F} = -\frac{\chi_0(\boldsymbol{k}, \mathrm{i}\omega)}{2}\left\{\langle D\rangle - \langle D^2\rangle N_F - \langle D^2\rangle \sum_{\boldsymbol{q},|\xi_q|\leqslant\varepsilon_F} \frac{1-2n_F(\xi_q)}{\mathrm{i}\omega - \xi_q}\right\}. \tag{22}$$

Now, using equation (21) in equation (14), i.e. $\Gamma_c^{(1)}(\boldsymbol{p}, \mathrm{i}\omega; \boldsymbol{k}, \mathrm{i}\omega')$ in equation (14) is replaced by $\Gamma_c^{(1)}(\boldsymbol{p}, \mathrm{i}\omega'; \boldsymbol{k}, \mathrm{i}\omega')$, and noting that

$$2\sum_{\boldsymbol{p}} \chi^0_{\boldsymbol{pk}}(\omega)\,\Delta\Gamma_c(\boldsymbol{p}, \xi_{\boldsymbol{p}-\boldsymbol{k}} + \mathrm{i}\omega; \boldsymbol{k}, \mathrm{i}\omega) \approx \chi_0(\boldsymbol{k}, \mathrm{i}\omega)\langle\Delta\Gamma_c^{(1)}(\boldsymbol{p}, \xi_{\boldsymbol{p}-\boldsymbol{k}} + \mathrm{i}\omega; \boldsymbol{k}, \mathrm{i}\omega)\rangle_{|\boldsymbol{p}|=p_F}$$

the irreducible charge-density response function can be expressed by

$$\tilde{\chi}_c(\boldsymbol{k}, \mathrm{i}\omega) = \frac{\chi_0(\boldsymbol{k}, \mathrm{i}\omega)}{1 - \langle\Delta\Gamma_c^{(1)}(\boldsymbol{p}, \xi_{\boldsymbol{p}-\boldsymbol{k}} + \mathrm{i}\omega; \boldsymbol{k}, \mathrm{i}\omega)\rangle_{|\boldsymbol{p}|=p_F}}. \tag{23}$$

Finally, using equation (22) to replace $\langle\Delta\Gamma_c^{(1)}(\boldsymbol{p}, \xi_{\boldsymbol{p}-\boldsymbol{k}} + \mathrm{i}\omega; \boldsymbol{k}, \mathrm{i}\omega)\rangle_{|\boldsymbol{p}|=p_F}$ in equation (23), after analytical continuation ($\mathrm{i}\omega \to \omega + \mathrm{i}\delta$) it follows that

$$\tilde{\chi}_c(\boldsymbol{k}, \omega) = \frac{\chi_0(\boldsymbol{k}, \omega_0)}{1 + [A_c - B_c(\omega)]\chi_0(\boldsymbol{k}, \omega)} \tag{24a}$$

where

$$B_c(\omega) = \tfrac{1}{2}\langle D^2(\boldsymbol{p}-\boldsymbol{q})\rangle \sum_{\boldsymbol{q},|\xi_q|\leqslant\varepsilon_F} \frac{1-2n_F(\xi_q)}{\omega - \xi_q + \mathrm{i}\delta}$$

$$A_c = \tfrac{1}{2}[\langle D(\boldsymbol{p}-\boldsymbol{p}')\rangle - \langle D^2(\boldsymbol{p}-\boldsymbol{q})\rangle N_F]. \tag{24b}$$

In equation (24) the contribution of the screened exchange interaction in the first order and screened direct interaction in the second order to the vertex correction is given by the term A_c, whereas $B_c(\omega)$ represents the contribution from the correlations in the 'Cooper' channel. In the high-density limit or for weak interelectron coupling ($\langle D\rangle N_F \ll 1$) the effect of the correction due to the exchange interaction is larger than that from the correlations in the 'Cooper' channel ($A_c \gg |B_c(0)|$). The effect of the vertex correction on $\tilde{\chi}_c(\boldsymbol{k}, \omega)$ in this case is small ($\Gamma_c \approx 1$) and $\tilde{\chi}_c(\boldsymbol{k}, \omega) \approx \chi_0(\boldsymbol{k}, \omega)$. In the low-density limit or for strong interelectron coupling ($\langle D\rangle N_F \approx 1$) the effect of the exchange corrections is almost zero, $A_c \approx 0$, because the second-order direct term almost compensates for the first-order exchange term. Only correlations in the 'Cooper' channel exist. Hence, $A_c \ll |B_c(0)|$. In this case the vertex correction in the particle–hole channel is large, $\Gamma_c(p_F, \omega \approx 0) \gg 1$ for low frequencies, while the frequency dependence disappears, $\Gamma_c(p_F, \omega) \approx 1$, for $\omega \geqslant \varepsilon_F$. Thus, in the case of intermediate or strong coupling, the correlations in the 'Cooper' channel are important.

The effect of the vertex correction on $\tilde{\chi}_c(\boldsymbol{k},\omega)$ is also significant. The irreducible response in the charge-density channel, using equation (24), can be rewritten as

$$\tilde{\chi}_c(\boldsymbol{k},\omega)_{|\omega<v_Fk} = \mathrm{Re}[\tilde{\chi}_c(\boldsymbol{k},\omega)_{|\omega<v_Fk}] + \mathrm{i}\,\mathrm{Im}[\tilde{\chi}_c(\boldsymbol{k},\omega)_{|\omega<v_Fk}] \tag{25}$$

where

$$\mathrm{Re}[\tilde{\chi}_c(\boldsymbol{k},\omega)_{|\omega<v_Fk}] \approx -\frac{N_F}{1+F_0^s(\omega)} \tag{26}$$

and

$$\mathrm{Im}[\tilde{\chi}_c(\boldsymbol{k},\omega)_{|\omega<vFk}] \approx -\frac{N_F}{(1+F_0^s(\omega))^2}\left\{\frac{\omega}{v_Fk}+\frac{\pi}{4}N_F^2\langle D^2\rangle\tanh\left(\frac{\omega}{2T}\right)\right\} \tag{27}$$

with $F_0^s(\omega) = -N_F[A_c - \mathrm{Re}\,B_c(\omega)]$ and $\mathrm{Re}[B_c(\omega)] \approx -\frac{1}{2}N_F\langle D^2\rangle\ln(\varepsilon_F/\max\{\omega,T\})$. In addition, the relation between $K^{\sigma\sigma'}(p,p')$, the kernel of the interaction, and the Landau Fermi-liquid interaction function $f^{\sigma\sigma'}(\boldsymbol{p},\boldsymbol{p}')$ gives $Z^{-1}(0)\langle f^{\uparrow\uparrow}_{\boldsymbol{p},\boldsymbol{p}'} + f^{\uparrow\downarrow}_{\boldsymbol{p},\boldsymbol{p}'}\rangle = -2[A_c - B_c(0)]$, where $\langle\ldots\rangle$ denotes the angular average over the Fermi surface as before. As seen, in the static limit, equation (26) turns into the result of Landau's Fermi-liquid theory [25, 26] with $F_0^s(0)$ being the Landau Fermi-liquid parameter in the charge channel at the zeroth frequency. Thus, $F_0^s(\omega)$ is the frequency-dependent Landau Fermi-liquid parameter in the charge channel. In addition, as seen, equation (27) incorporates both the behaviour proposed by Varma *et al*, i.e. $\mathrm{Im}\,\chi \sim -\omega/T$, and the standard Fermi-liquid result, $\mathrm{Im}\,\chi \sim -\omega/v_Fk$.

3. Response in the spin channel

Now, let us evaluate the response in the spin channel. Note that $D(k)$ depends on momentum only in the particle–hole channel as before. Therefore $K_s(p,p') = D(\boldsymbol{p}-\boldsymbol{p}',0)$ in equation (6*b*). We can carry out the average over the angle between $\boldsymbol{p}$ and $\boldsymbol{p}'$ in equation (6*b*) to get the solutions to equations (7) and (8) for the vertex and response functions, respectively, in the spin-density channel. In the approximation of the angular average, $K_s(p,p') = D(\boldsymbol{p}-\boldsymbol{p}',0) \approx \langle D(\boldsymbol{p}-\boldsymbol{p}')\rangle$, the vertex function in the spin channel depends on the momentum transfer only, namely $\Gamma_s(p,k) = \Gamma_s(k) = 1/[1+\langle K_s(\boldsymbol{p}-\boldsymbol{p}')\rangle\chi_0(k)/2]$ in equation (7). Thus, taking into account this $\Gamma_s(k)$ in equation (8), the irreducible polarizability in the spin-density channel is derived as

$$\tilde{\chi}_s(\boldsymbol{k},\omega) = \chi_0(\boldsymbol{k},\omega)/[1+\tfrac{1}{2}\langle D(\boldsymbol{p}-\boldsymbol{p}')\rangle\chi_0(\boldsymbol{k},\omega)]. \tag{28}$$

In the static and long-wavelength limit, equation (28) turns into the form of the well known result of the Landau Fermi-liquid theory [25, 26], $\tilde{\chi}_s(0,0) = -N_F/(1+F_0^a)$, where $F_0^a = -\langle D(\boldsymbol{p}-\boldsymbol{p}')\rangle N_F/2$ is the Landau Fermi-liquid parameter in the spin channel.

Now, as an example, let us evaluate F_0^a in a layered 2D Fermi gas with the isotropic electron spectrum in any of layers, i.e. $\varepsilon_{\boldsymbol{p}} = \boldsymbol{p}^2/2m^*$—the 2D single-particle energy. The equation $D(\boldsymbol{k}) = V(\boldsymbol{k})/[1-V(\boldsymbol{k})\chi_0(\boldsymbol{k},0)]$ was then used. It corresponds to the RPA for $D(k)$. Note that the bare Coulomb interaction $V(\boldsymbol{k})$, here in a layered system [27] is given by

$$V(\boldsymbol{k}) = V_0(k_\parallel)\frac{\sinh(ck_\parallel)}{\cosh(ck_\parallel)-\cos(ck_z)} = V_0(k_\parallel)f(\boldsymbol{k}) \tag{29}$$

where $k_\parallel$ and k_z are the momentum components in a plane and in the direction normal to it, respectively, $V_0(k_\parallel) = 2\pi e^2/\kappa k_\parallel$ is the bare Coulomb interaction in a pure 2D case with

the dielectric constant κ of the lattice background, and $f(\boldsymbol{k})$ is the form factor of a layered 2D system. Thus, we have

$$F_0^a = -\frac{cm^*}{(2\pi)^3}\int_{-\pi/c}^{\pi/c} \mathrm{d}p_z' \int_0^{2\pi} \mathrm{d}\varphi\, D(\boldsymbol{p}-\boldsymbol{p}')_{\|\boldsymbol{p}|\approx|\boldsymbol{p}'|\approx p_F} = -\frac{\alpha}{\pi}F(\alpha,\zeta) \qquad (30)$$

where

$$F(\alpha,\zeta) = \int_0^1 \mathrm{d}x\{(1-x^2)[x^2 + 2\alpha x\coth(\zeta x) + \alpha^2]\}^{-1/2} \qquad (31)$$

in which $\boldsymbol{k}_\|^2 = |\boldsymbol{p}_\| - \boldsymbol{p}_\|'|^2 = 2p_F^2(1-\cos\varphi)$ was used, $\alpha = e^2/\kappa v_F$ is the interelectron interaction constant with $v_F = p_F/m^*$ (m^* is the electron effective or band mass) and the dielectric constant κ, and $\zeta = 2p_F c$ with the 2D Fermi momentum $p_F = \sqrt{2\pi n_s}$ and the interlayer spacing c. Also, α is related to the dimensionless density parameter r_s by the relation $r_s = \sqrt{2}\alpha$. It follows from equation (31) that $F_0^a = -\mu_c$, where μ_c is the interelectron Coulomb repulsion parameter [28] in the RPA and its maximum value is $F_0^a = -\mu_c = -\frac{1}{2}$ for $\alpha \gg 1$, and that $F_0^a = -(\alpha/\pi)\ln(2/\alpha)$ in the case of the high-density limit ($\alpha \ll 1$) and for a large interlayer spacing ($p_F c \gg 1$). In addition, $\langle D\rangle = 2e^2F(\alpha,\zeta)/\kappa p_F$ is obtained in equation (31) and can be used, for example, in equation (24*b*) and elsewhere. Moreover, F_0^a in equation (31) decreases with decrease in interlayer spacing c, when $c < a_B^*$, namely $F_0^a \approx -1/2\sqrt{1 + a_B^*/c}$, where $a_B^* = \kappa/e^2m^*$ is the effective Bohr radius.

Thus, from equations (28) and (30), the response in the spin channel, at least in the RPA, complies with the result of the conventional Fermi-liquid theory:

$$\mathrm{Im}[\tilde{\chi}_s(\boldsymbol{k},\omega)_{|\omega<v_Fk|}] \approx -\frac{N_F}{(1+F_0^a)^2}\frac{\omega}{v_Fk}. \qquad (32)$$

Equation (32) leads to the well known Korringa law [29], i.e.

$$T_1^{-1} \sim -\lim_{\omega\to 0}\left(\frac{T}{\omega}\sum_{\boldsymbol{k}}\mathrm{Im}[\tilde{\chi}_s(\boldsymbol{k},\omega)]\right) \sim T.$$

Thus, equation (32) disagrees with equation (1) in the spin channel and does not comply with the MFL model. This means that equation (32) does not include the effect of the virtual pair excitations and, hence, cannot describe the deviation from the Korringa law in cuprates. It is apparently necessary to consider the effect of the virtual pair excitations on the vertex correction in the spin channel. Therefore, in this case we have to evaluate $K_s(p,p')$, the kernel of interaction in the spin channel, in the higher orders beyond the RPA.

Let us assume that we have already evaluated $\Gamma_c(p,k)$, the vertex correction in the charge-density channel (the approximate analytical expression for $\Gamma_c(p,k)$ is given by equation (21)). Then, equation (4) for the single-particle self-energy containing the vertex correction in the charge channel is described by

$$\Sigma_\sigma(p) = \mathrm{i}\int \frac{\mathrm{d}^4k}{(2\pi)^4}G_\sigma(p-k)D_c(k)\Gamma_c(p,k)$$

where $D_c(k)$ is the boson propagator beyond the RPA. Now, we can evaluate $K^{\sigma\sigma'}(p,p')$, using the relation $K^{\sigma\sigma'}(p,p') = -\mathrm{i}\,\delta\Sigma_\sigma(p)/\delta G_{\sigma'}(p')$ as before. The expression for the kernel of interaction in the spin channel including the vertex correction $\Gamma_c(p,k)$ from the charge channel can be derived as $K_s(p,p') = D_c(p-p')\Gamma_c(p,p-p')$. It apparently differs from equation (6*b*), where $K_s(p,p') = D^{RPA}(p-p')$. The expression for $K_s(p,p')$ in the form of $K_s(p,p') = D_c(p-p')\Gamma_c(p,p-p')$, in fact, represents the leading contribution to

the interaction in the spin channel. It accounts for neither the higher-order contributions such as $U^2\tilde{\chi}_s(p-p')$, the contribution to the interaction in the spin channel from the paramagnon exchange [30] (where $U = \langle D(\boldsymbol{p}-\boldsymbol{p}')\rangle/2$ is the short-range exchange interaction), nor $\delta\Gamma_c(p,k)/\delta G_\sigma(p')$, the contribution coming from the functional derivative of the vertex function with respect to the Green function. Using previously obtained results for the vertex function (equation (21)) and the irreducible response function in the charge channel (equation (23)), the equation for the irreducible response function in the spin channel can be derived, in analogy to equation (23), as follows:

$$\tilde{\chi}_s(\boldsymbol{k},\mathrm{i}\omega) = \frac{\chi_0(\boldsymbol{k},\mathrm{i}\omega)}{1-\langle\Delta\Gamma_s^{(1)}(\boldsymbol{p},\xi_{\boldsymbol{p}-\boldsymbol{k}}+\mathrm{i}\omega;\boldsymbol{k},\mathrm{i}\omega)\rangle_{|\boldsymbol{p}|=p_F}} \tag{33}$$

where $\Delta\Gamma_s^{(1)}(\boldsymbol{p},\mathrm{i}\omega;\boldsymbol{k},\mathrm{i}\omega')$ is the vertex correction of the first order in the spin channel, and $\chi_0(\boldsymbol{k},\omega)$ is the free-particle response function as before. Using equation (12) with $K_s(p,p') = D_c(p-p')\Gamma_c(p,p-p')$ (in equation (12) $K_c(p,p')$ is replaced by $K_s(p,p')$), the vertex correction $\Delta\Gamma_s^{(1)}(\boldsymbol{p},\mathrm{i}\omega;\boldsymbol{k},\mathrm{i}\omega')$ of the first order, in the spin channel in equation (33) can be written as

$$\begin{aligned}\Delta\Gamma_s^{(1)}(\boldsymbol{p},\xi_{\boldsymbol{p}-\boldsymbol{k}}+\mathrm{i}\omega;\boldsymbol{k},\mathrm{i}\omega) &= -\sum_{\boldsymbol{p}'}\chi^0_{\boldsymbol{p}'\boldsymbol{k}}(\omega)K_s(\boldsymbol{p},\xi_{\boldsymbol{p}-\boldsymbol{k}}+\mathrm{i}\omega;\boldsymbol{p}',\xi_{\boldsymbol{p}'-\boldsymbol{k}}+\mathrm{i}\omega)\\ &= -\sum_{\boldsymbol{p}'}\chi^0_{\boldsymbol{p}'\boldsymbol{k}}(\omega)D_c(\boldsymbol{p}-\boldsymbol{p}',\xi_{\boldsymbol{p}-\boldsymbol{k}}-\xi_{\boldsymbol{p}'-\boldsymbol{k}})\\ &\quad\times\Gamma_c(\boldsymbol{p},\xi_{\boldsymbol{p}-\boldsymbol{k}}+\mathrm{i}\omega;\boldsymbol{p}-\boldsymbol{p}',\xi_{\boldsymbol{p}-\boldsymbol{k}}-\xi_{\boldsymbol{p}'-\boldsymbol{k}})\end{aligned} \tag{34}$$

where $\chi^0_{\boldsymbol{p}'\boldsymbol{k}}(\omega)$ is given by equation (13), $\Gamma_c(\boldsymbol{p},\mathrm{i}\omega;\boldsymbol{k},\mathrm{i}\omega)$ is the vertex function in the charge channel and is given by equation (21). In equation (34), $D_c(\boldsymbol{k},\omega)$ is the boson propagator beyond the RPA. It satisfies the Dyson equation (see $D(k)$ in equation (4)) and, therefore, incorporates the irreducible charge-density response function $\tilde{\chi}_c(\boldsymbol{k},\omega)$. In the case of the Coulomb interaction $D_c(\boldsymbol{k},\omega) = V(\boldsymbol{k})/[1-V(\boldsymbol{k})\tilde{\chi}_c(\boldsymbol{k},\omega)]$, where $V(\boldsymbol{k})$ is a bare Coulomb interaction (in the case of a layered 2D system, $V(\boldsymbol{k})$ is given by equation (29)), and $\tilde{\chi}_c(\boldsymbol{k},\omega)$ is the irreducible charge-density response function given by equation (23) or (24). Using equation (21) in equation (34), $\Delta\Gamma_s^{(1)}(\boldsymbol{p},\xi_{\boldsymbol{p}-\boldsymbol{k}}+\mathrm{i}\omega;\boldsymbol{k},\mathrm{i}\omega)$ can be represented by

$$\Delta\Gamma_s^{(1)}(\boldsymbol{p},\xi_{\boldsymbol{p}-\boldsymbol{k}}+\mathrm{i}\omega;\boldsymbol{k},\mathrm{i}\omega) = \Delta_{s1}+\Delta_{s2} \tag{35}$$

where

$$\Delta_{s1} = -\sum_{\boldsymbol{p}'}\chi^0_{\boldsymbol{p}'\boldsymbol{k}}(\omega)D_c(\boldsymbol{p}-\boldsymbol{p}',\xi_{\boldsymbol{p}-\boldsymbol{k}}-\xi_{\boldsymbol{p}'-\boldsymbol{k}}) \approx -\tfrac{1}{2}\langle D_c(\boldsymbol{p}-\boldsymbol{p}',0)\rangle\chi_0(\boldsymbol{k},\mathrm{i}\omega) \tag{36}$$

and

$$\begin{aligned}\Delta_{s2} &= -\sum_{\boldsymbol{p}'}\chi^0_{\boldsymbol{p}'\boldsymbol{k}}(\omega)\frac{D_c(\boldsymbol{p}-\boldsymbol{p}',\xi_{\boldsymbol{p}-\boldsymbol{k}}-\xi_{\boldsymbol{p}'-\boldsymbol{k}})\Delta\Gamma_c^{(1)}(\boldsymbol{p},\xi_{\boldsymbol{p}-\boldsymbol{k}}+\mathrm{i}\omega;\boldsymbol{p}-\boldsymbol{p}',\xi_{\boldsymbol{p}-\boldsymbol{k}}-\xi_{\boldsymbol{p}'-\boldsymbol{k}})}{1-\langle\Delta\Gamma_c^{(1)}(\boldsymbol{p}'',\xi_{\boldsymbol{p}''-\boldsymbol{p}+\boldsymbol{p}'}+\xi_{\boldsymbol{p}-\boldsymbol{k}}-\xi_{\boldsymbol{p}'-\boldsymbol{k}};\boldsymbol{p}-\boldsymbol{p}',\xi_{\boldsymbol{p}-\boldsymbol{k}}-\xi_{\boldsymbol{p}'-\boldsymbol{k}})\rangle_{|\boldsymbol{p}''|=p_F}}\\ &\approx -\left\langle\frac{D_c(\boldsymbol{p}-\boldsymbol{p}',0)}{1-\langle\Delta\Gamma_c^{(1)}(\boldsymbol{p}'',\xi_{\boldsymbol{p}''-\boldsymbol{p}+\boldsymbol{p}'};\boldsymbol{p}-\boldsymbol{p}',0)\rangle_{|\boldsymbol{p}''|=p_F}}\right\rangle\\ &\quad\times\sum_{\boldsymbol{p}'}\chi^0_{\boldsymbol{p}'\boldsymbol{k}}(\omega)\,\Delta\Gamma_c^{(1)}(\boldsymbol{p},\xi_{\boldsymbol{p}-\boldsymbol{k}}+\mathrm{i}\omega;\boldsymbol{p}-\boldsymbol{p}',\xi_{\boldsymbol{p}-\boldsymbol{k}}-\xi_{\boldsymbol{p}'-\boldsymbol{k}}).\end{aligned} \tag{37}$$

In equations (36) and (37) the angular average was made as before, and $D_c(\boldsymbol{k},\omega)\approx D_c(\boldsymbol{k},0)$ because $\omega = \xi_{\boldsymbol{p}-\boldsymbol{k}}-\xi_{\boldsymbol{p}'-\boldsymbol{k}}\to 0$ for $k\to 0$ and $|\boldsymbol{p}|\approx|\boldsymbol{p}'|\approx p_F$. Using equation (12) in equation (37), Δ_{s2} can be written as follows:

$$\begin{aligned}\Delta_{s2} &\approx \langle\tilde{D}_c(\boldsymbol{p}-\boldsymbol{p}',0)\rangle\sum_{\boldsymbol{p}',\boldsymbol{p}''}\chi^0_{\boldsymbol{p}'\boldsymbol{k}}(\omega)\chi^0_{\boldsymbol{p}'',\boldsymbol{p}-\boldsymbol{p}'}(\xi_{\boldsymbol{p}-\boldsymbol{k}}-\xi_{\boldsymbol{p}'-\boldsymbol{k}})\\ &\quad\times K_c(\boldsymbol{p},\xi_{\boldsymbol{p}-\boldsymbol{k}}+\mathrm{i}\omega;\boldsymbol{p}'',\xi_{\boldsymbol{p}''-\boldsymbol{p}+\boldsymbol{p}'}+\xi_{\boldsymbol{p}-\boldsymbol{k}}-\xi_{\boldsymbol{p}'-\boldsymbol{k}})\end{aligned} \tag{38}$$

where

$$\chi^0_{\boldsymbol{p}'',\boldsymbol{p}-\boldsymbol{p}'}(\xi_{\boldsymbol{p}-\boldsymbol{k}}-\xi_{\boldsymbol{p}'-\boldsymbol{k}})=\frac{n_F(\xi_{\boldsymbol{p}''})-n_F(\xi_{\boldsymbol{p}''-\boldsymbol{p}+\boldsymbol{p}'})}{\xi_{\boldsymbol{p}''}-\xi_{\boldsymbol{p}''-\boldsymbol{p}+\boldsymbol{p}'}-(\xi_{\boldsymbol{p}-\boldsymbol{k}}-\xi_{\boldsymbol{p}'-\boldsymbol{k}})}$$

and

$$\tilde{D}_c(\boldsymbol{k},\omega)=\frac{D_c(\boldsymbol{k},\omega)}{1-\langle\Delta\Gamma^{(1)}_c(\boldsymbol{p},\xi_{\boldsymbol{p}-\boldsymbol{k}}+\omega;\boldsymbol{k},\omega)\rangle_{|\boldsymbol{p}|=p_F}}. \tag{39}$$

Using equation (9) in equation (38), the contribution of the virtual pair excitations to equation (38) is given by the last term in equation (9) and can be represented by

$$\Delta^{pair}_{s2}\approx -2\langle\tilde{D}_c\rangle\langle D^2\rangle\sum_{\boldsymbol{p}',\boldsymbol{p}'',\boldsymbol{q}}\chi^0_{\boldsymbol{p}'\boldsymbol{k}}(\omega)\chi^0_{\boldsymbol{p}'',\boldsymbol{p}-\boldsymbol{p}'}(\xi_{\boldsymbol{p}-\boldsymbol{k}}-\xi_{\boldsymbol{p}'-\boldsymbol{k}})$$
$$\times\frac{1-n_F(\xi_{\boldsymbol{q}})-n_F(\xi_{\boldsymbol{p}''+\boldsymbol{p}-\boldsymbol{q}})}{\mathrm{i}\omega+\xi_{\boldsymbol{p}-\boldsymbol{k}}+\xi_{\boldsymbol{p}''-\boldsymbol{p}+\boldsymbol{p}'}+\xi_{\boldsymbol{p}-\boldsymbol{k}}-\xi_{\boldsymbol{p}'-\boldsymbol{k}}-\xi_{\boldsymbol{q}}-\xi_{\boldsymbol{p}''+\boldsymbol{p}-\boldsymbol{q}}} \tag{40}$$

where $\langle\tilde{D}_c\rangle=\langle\tilde{D}_c(\boldsymbol{p}-\boldsymbol{p}',0)\rangle$. We can perform the average over the Fermi surface in equation (40) with respect to $\boldsymbol{p}$ in analogy to equation (19) and the summation (integration) over $\boldsymbol{p}'$ and $\boldsymbol{p}''$ in equation (40) noting that $\xi_{\boldsymbol{p}-\boldsymbol{k}}-\xi_{\boldsymbol{p}'-\boldsymbol{k}}\approx 0$ since $\boldsymbol{p}-\boldsymbol{p}'\approx\boldsymbol{k}\to 0$, and that $\xi_{\boldsymbol{p}-\boldsymbol{k}}+\xi_{\boldsymbol{p}''-\boldsymbol{p}+\boldsymbol{p}'}\approx\xi_{\boldsymbol{p}-\boldsymbol{k}}+\xi_{\boldsymbol{p}''-\boldsymbol{k}}\approx 0(\ll\omega)$ because $\boldsymbol{p}=-\boldsymbol{p}''$ and $|\boldsymbol{p}|\approx p_F$.

Then, after the average over the Fermi surface, equation (40) can be converted to

$$\langle\Delta^{pair}_{s2}\rangle\approx\tfrac{1}{2}\langle\tilde{D}_c\rangle\langle D^2\rangle N_F\chi_0(\boldsymbol{k},\mathrm{i}\omega)\sum_{\boldsymbol{q},|\xi_q|\leqslant\varepsilon_F}\frac{1-2n_F(\xi_{\boldsymbol{q}})}{\mathrm{i}\omega-2\xi_{\boldsymbol{q}}}. \tag{41}$$

Finally, using equations (9) and (36)–(41), we have

$$\langle\Delta\Gamma^{(1)}_s(\boldsymbol{p},\xi_{\boldsymbol{p}-\boldsymbol{k}}+\omega;\boldsymbol{k},\omega)\rangle_{|\boldsymbol{p}|=p_F}\approx-[A_s-B_s(\omega)]\chi_0(\boldsymbol{k},\omega) \tag{42}$$

where

$$A_s=\tfrac{1}{2}[\langle D_c(\boldsymbol{p}-\boldsymbol{p}',0)\rangle+\langle\tilde{D}_c(\boldsymbol{p}-\boldsymbol{p}',0)\rangle N_F A_c] \tag{43}$$

and

$$B_s(\omega)=\tfrac{1}{2}\langle\tilde{D}_c(\boldsymbol{p}-\boldsymbol{p}',0)\rangle\langle D^2(\boldsymbol{p}-\boldsymbol{q})\rangle N_F\sum_{\boldsymbol{q},|\xi_q|\leqslant\varepsilon_F}\frac{1-2n_F(\xi_{\boldsymbol{q}})}{\omega-2\xi_{\boldsymbol{q}}+\mathrm{i}\delta} \tag{44}$$

and A_c is given in equation (24*b*). Now, using equation (42) with equations (43) and (44) in equation (33), the irreducible spin-density response function can finally be expressed by

$$\tilde{\chi}_s(\boldsymbol{k},\omega)=\frac{\chi_0(\boldsymbol{k},\omega)}{1+[A_s-B_s(\omega)]\chi_0(\boldsymbol{k},\omega)} \tag{45}$$

where the parameters A_s and $B_s(\omega)$ are given by equations (43) and (44), respectively.

Further, equation (45) can also be represented in a form similar to equation (25). Thus, we have

$$\tilde{\chi}_s(\boldsymbol{k},\omega)_{|\omega<v_Fk}=\mathrm{Re}[\tilde{\chi}_s(\boldsymbol{k},\omega)_{|\omega<v_Fk}]+\mathrm{i}\,\mathrm{Im}[\tilde{\chi}_s(\boldsymbol{k},\omega)_{|\omega<v_Fk}] \tag{46}$$

where

$$\mathrm{Re}[\tilde{\chi}_s(\boldsymbol{k},\omega)_{|\omega<v_Fk}]\approx-\frac{N_F}{1+F^a_0(\omega)} \tag{47}$$

and

$$\mathrm{Im}[\tilde{\chi}_s(\boldsymbol{k},\omega)_{|\omega<v_Fk}]\approx-\frac{N_F}{(1+F^a_0(\omega))^2}\left\{\frac{\omega}{v_Fk}+\frac{\pi}{8}N_F^3\langle\tilde{D}_c\rangle\langle D^2\rangle\tanh\left(\frac{\omega}{4T}\right)\right\} \tag{48}$$

with $F_0^a(\omega) = -N_F\{A_s - \mathrm{Re}[B_s(\omega)]\}$ being the Landau Fermi-liquid parameter in the spin channel, and $\mathrm{Re}[B_s(\omega)] \approx -\frac{1}{4}N_F^2\langle\tilde{D}_c\rangle\langle D^2\rangle \ln(\varepsilon_F/\max\{\omega/2, T\})$.

In addition, one can show that the expression $A_s - B_s(0)$ is related to the Landau Fermi-liquid interaction function $f^{\sigma\sigma'}(\boldsymbol{p}, \boldsymbol{p}')$ as $2[A_s - B_s(0)] = -Z^{-1}(0)\langle f^{\uparrow\uparrow}_{\boldsymbol{p},\boldsymbol{p}'} - f^{\uparrow\downarrow}_{\boldsymbol{p},\boldsymbol{p}'}\rangle$. It can be seen that, in the static limit, equation (47) gives rise to the result of the Landau Fermi-liquid theory [25, 26] with $F_0^a(0)$ being the Landau Fermi-liquid parameter in the spin channel at the zeroth frequency. Thus, in the case of intermediate and strong coupling, $F_0^a(\omega)$ becomes the frequency-dependent Landau Fermi-liquid parameter in the spin channel, in contrast with equation (30) where in the RPA this parameter is frequency independent. In addition, equation (48) contains both the behaviour suggested by Varma *et al* i.e. $\mathrm{Im}\,\chi \sim -\omega/T$, and the standard Fermi-liquid result $\mathrm{Im}\,\chi \sim -\omega/v_F k$. It is concluded from equation (48) that the contribution of the term $\sim -\omega/T$ to the response function in the spin channel is much smaller than that in the charge channel because $\mathrm{Im}\,\tilde{\chi}_s \sim -(\pi/8)N_F\lambda^3\tanh(\omega/4T)$, where $\lambda \sim N_F\langle D\rangle$, whereas in the charge-density channel it is $\mathrm{Im}\,\tilde{\chi}_c \sim -(\pi/4)N_F\lambda^2\tanh(\omega/2T)$.

Now, it is possible to estimate the inverse nuclear-spin relaxation time using equation (48). It can be shown that

$$T_1^{-1} \sim -\lim_{\omega\to 0}\left(\frac{T}{\omega}\sum_{\boldsymbol{k}}\mathrm{Im}[\tilde{\chi}_s(\boldsymbol{k},\omega)]\right) \approx \tilde{\chi}_s^2(0,0)\left(T + \frac{\pi}{16}\lambda_s^3\varepsilon_F\right) \tag{49}$$

where the interelectron coupling constant in the spin channel $\lambda_s = N_F^3\sqrt{\langle\tilde{D}_c\rangle\langle D^2\rangle}$ is introduced, the spin susceptibility $\tilde{\chi}_s(0,0)$ of the Fermi liquid is given by equation (47) and ε_F is the Fermi energy. It is apparent that equation (49), which shows the deviation from the Korringa law due to the virtual pair excitations, can fit the experimental data for cuprates, where experiment for the inverse nuclear relaxation time shows the temperature dependence $T_1^{-1} \sim aT + b$ with an almost temperature-independent term b [9, 31]. The comparison of equation (49) with experiments for cuprates gives $a \propto \tilde{\chi}_s^2(0,0)$ and $b \propto a(\pi/16)\lambda_s^3\varepsilon_F$.

4. Discussion

Now, as an example, we can estimate the interelectron interaction constants, such as $\langle D^2\rangle$, $\langle D_c\rangle$ and $\langle\tilde{D}_c\rangle$, in a layered 2D system. Firstly, we evaluate $\langle D^2\rangle$ or $\langle D^2\rangle N_F$ because $\langle D\rangle = 2e^2F(\alpha,\zeta)/\kappa p_F$ can be evaluated in terms of equation (31). The angular average in analogy to equation (30) leads to the expression

$$\langle D^2(\boldsymbol{p}-\boldsymbol{p}')\rangle N_F = 2\alpha\frac{e^2}{\kappa p_F}\tilde{F}(\alpha,\xi) \tag{50a}$$

where

$$\tilde{F}(\alpha,\zeta) = \int_0^1 \frac{\mathrm{d}x}{\sqrt{1-x^2}}\frac{x\coth(\zeta x)+\alpha}{[x^2+2\alpha x\coth(\zeta x)+\alpha^2]^{3/2}} \tag{50b}$$

and $\alpha = e^2/\kappa v_F$ is the interelectron interaction constant as before, $N_F = m^*/\pi$ is the 2D density of states, and $\zeta = 2p_F c$ with interlayer spacing c. It is interesting to note that $\tilde{F}(\alpha,\zeta)$ behaves in the limiting cases as follows. In the case of a large interlayer spacing $\zeta \gg 1$ and weak interelectron coupling of high-density limit ($\alpha \ll 1$), $\tilde{F}(\alpha,\zeta) \approx 1/\alpha$ while, in the case of strong coupling or low-density limit ($\alpha \gg 1$), $\tilde{F}(\alpha,\zeta) \approx \pi/(2\alpha^2)$. The value of $\tilde{F}(\alpha,\zeta)$ weakly depends on the interlayer spacing when $c \gg a_B^*$, and it decreases with decrease in c when $c < a_B^*$, namely $\tilde{F}(\alpha,\zeta) \approx (\pi/2\alpha^2)(1+a_B^*/2c)/(1+a_B^*/c)^{3/2}$. This is analogous to the c-dependence of $F(\alpha,\zeta)$ from equation (31). In contrast with the behaviour

of $\tilde{F}(\alpha, \zeta)$ in the limiting cases, from equation (31), $F(\alpha, \zeta) \approx \ln(2/\alpha)$ in the case of a large interlayer separation $\zeta \gg 1$ and for weak coupling $\alpha \ll 1$ while $F(\alpha, \zeta) \approx \pi/(2\alpha)$ in the case of strong coupling $\alpha \gg 1$. Now, using equation (50*a*), we can estimate the value of λ^2, defined as $N_F^2\langle D^2\rangle$, in a layered 2D system. In the case of weak coupling $\alpha \ll 1$, $\lambda^2 = N_F^2\langle D^2\rangle = (2/\pi)\alpha^2\tilde{F}(\alpha, \zeta) \approx (2/\pi)\alpha \ll 1$. This means that the contribution of the virtual pair excitations to the response in the charge channel becomes less important in the case of weak coupling or in the high-density limit ($\alpha \ll 1$). However, in the case of intermediate coupling ($\alpha \approx 1$) and for strong coupling ($\alpha \gg 1$) it follows that $\lambda \approx 1$. Therefore, the contribution of the term $\sim \tanh(\omega/2T)$ in equation (27) should not be ignored. This may explain why no marginal behaviour is observed in the conventional superconductors while it is the preliminary characteristics in cuprates.

Secondly, we consider $\langle D_c\rangle$, and $\langle \tilde{D}_c\rangle$ in a layered 2D system. First of all, we estimate the condition of instability of the Fermi liquid with respect to the charge-density wave instability, i.e. the condition of instability of the zero-sound mode [17, 25, 26] which is determined by the condition $F_0^s(0) \leqslant -1$. From equation (26), using equations (31) and (50*a*), we have the critical temperature

$$T_{cs} \approx 1.13\varepsilon_F \exp\left\{-\frac{1}{\alpha\tilde{F}(\alpha, \zeta)}\left(\frac{\pi}{\alpha} - F(\alpha, \zeta) + \alpha\tilde{F}(\alpha, \zeta)\right)\right\} \tag{51}$$

at which the zero-sound mode becomes unstable. Equation (51) allows us to obtain T_{cs} in the limiting cases. For example, in the case of the high-density limit or weak coupling ($\alpha \ll 1$) and for a large interlayer spacing ($\zeta = 2p_F c \gg 1$), $T_{cs} \sim \varepsilon_F \exp(-\pi/\alpha)$ is very low. In the low-density limit or for strong interelectron coupling ($\alpha \gg 1$), $T_{cs} \approx 1.13\varepsilon_F \exp(-2) \approx 0.153\varepsilon_F \approx 0.48n_s/m^*$. These are in line with our previous estimates [22]. Equation (51) determines a temperature region where correlations in the particle–hole channel become significant. Further, in equation (34) or equation (36), $D_c(\boldsymbol{k}, \omega)$ is the screened Coulomb interaction given by $D_c(\boldsymbol{k}, \omega) = V(\boldsymbol{k})/\varepsilon(\boldsymbol{k}, \omega) = V(\boldsymbol{k})/[1 - V(\boldsymbol{k})\tilde{\chi}_c(\boldsymbol{k}, \omega)]$, where $\varepsilon(\boldsymbol{k}, \omega)$ is the dielectric response function, $V(\boldsymbol{k})$ is a bare Coulomb interaction (in the case of a layered 2D system, $V(\boldsymbol{k})$ is given by equation (29)), and $\tilde{\chi}_c(\boldsymbol{k}, \omega)$ is the irreducible charge-density response function which, in the long-wavelength limit ($k \ll 2p_F$), is given by equations (24) or (26). It is also understood that, with increase on the wavevector $|\boldsymbol{k}|$, the parameter $F_0^s(\omega)$ in equation (26) should decrease because $D(\boldsymbol{k})$ in equation (24*b*) decreases with increase in k when $k > 2p_F$. It is possible to approximate the k-dependence of $F_0^s(\omega)$ in the Hubbard-like manner. This implies that in equation (50) for $\langle D^2\rangle N_F$ or $\langle D\rangle = 2e^2F(\alpha, \zeta)/\kappa p_F$ we can replace p_F in the denominator by $\sqrt{k^2 + p_F^2}$, where k is in the in-plane wavevector. It can be shown, using equations (26), (31) and (50), that in this approximation $F_0^s(k, \omega)$ turns into the form

$$F_0^s(k, \omega) \approx -\frac{\alpha P(\omega, T)}{\sqrt{1 + k^2/p_F^2}} \tag{52}$$

where $P(\omega, T) = \pi^{-1}[F(\alpha, \zeta) - \alpha\tilde{F}(\alpha, \zeta) + \alpha\tilde{F}(\alpha, \zeta)\ln(\varepsilon_F/x)]$ is a function of frequency, temperature, interelectron interaction constant α and interlayer spacing c related to ζ by $\zeta = 2p_F c$, and $x = \max\{\omega, T\}$. Equation (52), in fact, qualitatively describes the k-dependence of $F_0^s(k, \omega)$, and actually does not affect the final results too much. Nevertheless, it is convenient to introduce such a k-dependence. Thus, using equation (52) in equation (26), and employing the angular average in analogy to equation (30), $\langle D_c(\boldsymbol{p} - \boldsymbol{p}', 0)\rangle$ can be

derived as

$$\langle D_c(\boldsymbol{p}-\boldsymbol{p}',0)\rangle = \frac{2e^2}{\kappa p_F}\lambda(\alpha,\zeta) \tag{53a}$$

where

$$\lambda(\alpha,\zeta) = \int_{\min\{1,(1/2)\,\mathrm{Re}\,\sqrt{P_0^2\alpha^2-1}\}}^{1} \Phi(x)\,\mathrm{d}x - \int^{\min\{1,(1/2)\,\mathrm{Re}\,\sqrt{P_0^2\alpha^2-1}\}} \Phi(x)\,\mathrm{d}x \tag{53b}$$

$P_0 = P_0(\omega=0,T)$ and $\Phi(x) = \{(1-x^2)[x^2+\tilde{\alpha}^2+2\tilde{\alpha}x\coth(\zeta x)]\}^{-1/2}$, with the effective coupling parameter $\tilde{\alpha} = \alpha/(1-\alpha P_0/\sqrt{1+4x^2})$. It follows from equation (53*b*) that, in the case of weak coupling or in the high-density limit ($\alpha \ll 1$), $\lambda(\alpha,\zeta) = F(\alpha,\zeta)$, and equation (53*a*) exactly coincides with that in the RPA, i.e. $\langle D_c(\boldsymbol{p}-\boldsymbol{p}',0)\rangle = \langle D(\boldsymbol{p}-\boldsymbol{p}')\rangle$ in this case. In the case of strong interelectron coupling or in the low-density limit ($\alpha \gg 1$), $\lambda(\alpha,\zeta)(<0)$ is negative and its absolute value may be large. It is seen from equation (53*b*) that, for a large interlayer spacing, $\lambda(\alpha,\zeta) \approx -1.33P_0 \approx -1.33$($P_0 \approx 1$ was assumed) and $|\lambda(\alpha,\zeta)|$ in this case also increases with decrease in temperature because of the temperature dependence of P_0. It is interesting to note that in the case of strong coupling the value of $|\lambda(\alpha,\zeta)|$ depends on the interlayer spacing c, increases as it decreases, and becomes large for $c \approx 1/p_F$. The negative value of $\lambda(\alpha,\zeta)$ in the case of strong coupling corresponds to the strong attraction due to the exchange–correlation effects in the electron–hole channel. The fact that such an attraction (negative value of $\lambda(\alpha,\zeta)$) leads to the existence of the undamped zero-sound spin wave in the correlated Fermi liquid will be discussed later.

Now let us evaluate $\langle\tilde{D}_c\rangle = \langle\tilde{D}_c(\boldsymbol{p}-\boldsymbol{p}',0)\rangle$. Using equation (22) in equation (39) and taking into account equations (26) and (52), $\tilde{D}_c(\boldsymbol{k},\omega)$ can be written as

$$\tilde{D}_c(\boldsymbol{k},\omega) = \frac{V(\boldsymbol{k})}{1-V(\boldsymbol{k})[1-G_c(\boldsymbol{k},\omega)]\chi_0(\boldsymbol{k},\omega)} \tag{54}$$

where $G_c(\boldsymbol{k},\omega) = V^{-1}(\boldsymbol{k})[A_c - B_c(\omega)] \approx -V^{-1}(\boldsymbol{k})N_F^{-1}F_0^s(k,\omega) = P(\omega,T)G_H(\boldsymbol{k})$ is introduced as the local field factor in the charge channel. $P(\omega,T)$ is defined in equation (52). $G_H(\boldsymbol{k}) = k/(2f(\boldsymbol{k})\sqrt{k^2+p_F^2})$, [32] is the well-known Hubbard-like local field factor, where $f(\boldsymbol{k})$ is the form factor of a layered 2D system given in equation (29). The angular average in equation (54) for $\tilde{D}_c(\boldsymbol{p}-\boldsymbol{p}',0)$, in analogy to equation (30), leads to the expression

$$\langle\tilde{D}_c(\boldsymbol{p}-\boldsymbol{p}',0)\rangle = \frac{2e^2}{\kappa p_F}\mu(\alpha,\zeta) \tag{55a}$$

where

$$\mu(\alpha,\zeta) = \int_0^1 \frac{\mathrm{d}x}{\sqrt{1-x^2}} \times \frac{1}{\sqrt{x^2(1-\alpha P_0/\sqrt{1+4x^2})^2 + 2\alpha x(1-\alpha P_0/\sqrt{1+4x^2})\coth(\zeta x)+\alpha^2}} \tag{55b}$$

and $P_0 = P(\omega=0,T)$ as before. From equation (55*b*) μ can be analytically calculated in the limiting cases. For example, in the case of the high-density limit ($\alpha \ll 1$) and for a large interlayer spacing $\zeta = 2p_Fc \gg 1$, $\mu \approx \ln(2/\alpha)$ and we have the RPA result $\mu(\alpha,\zeta) = F(\alpha,\zeta)$. In fact, this region of the carrier density corresponds to a normal metal. In the low-density limit ($\alpha \gg 1$)), the value of μ depends on P_0; if $P_0 = 1$, corresponding to

the Hubbard approximation, $\mu \approx 0.8\pi/\alpha$, whereas, in the RPA (which corresponds $P_0 = 0$ in equation (55*b*)) $\mu = 0.5\pi/\alpha$. These conclusions confirm our earlier results shown in [22] in a different way.

Now, using equations (50)–(55) we can evaluate A_s and $B_s(\omega)$ included in equation (45) in the spin channel for a layered 2D system as follows:

$$A_s N_F = \frac{\alpha}{\pi}\left\{\lambda(\alpha,\pi) + \frac{\alpha}{\pi}\mu(\alpha,\zeta)[F(\alpha,\zeta) - \alpha\tilde{F}(\alpha,\zeta)]\right\} \tag{56}$$

and

$$N_F B_s(\omega) = \frac{2}{\pi^2}\alpha^3\mu(\alpha,\zeta)\tilde{F}(\alpha,\zeta)N_F^{-1}\sum_{q,|\xi_q|\leqslant\varepsilon_F}\frac{1-2n_F(\xi_q)}{\omega - 2\xi_q + \mathrm{i}\delta} \tag{57}$$

where $\lambda(\alpha,\zeta)$, $\mu(\alpha,\zeta)$, $F(\alpha,\zeta)$ and $\tilde{F}(\alpha,\zeta)$ are given by equations (53*b*), (55*b*), (31) and (50*b*), respectively. Furthermore, using equations (55) and (50), the interelectron coupling constant λ_s in the spin channel, which was introduced in equations (49), can be expressed by

$$\lambda_s^3 = \frac{4}{\pi^2}\alpha^3\mu(\alpha,\zeta)\tilde{F}(\alpha,\zeta) \tag{58}$$

where $\mu(\alpha,\zeta)$ and $\tilde{F}(\alpha,\zeta)$ are defined as before. It is concluded from equation (58) that, in the weak-coupling limit ($\alpha \ll 1$), $\lambda_s^3 \approx (4/\pi^2)\alpha^2\ln(2/\alpha) \ll 1$ is very small, and the contribution of the virtual pair excitations to the nuclear-spin relaxation time is negligible. The Koringa law is well observed in this case. In the strong-coupling limit ($\alpha \gg 1$), $\lambda_s^3 \approx 1$ and the deviation from the Korringa law is appreciable.

In addition, it is worthwhile to point out that, in the strong-coupling limit ($\alpha \gg 1$), as seen from equations (56) and (57), $N_F A_s \approx (\alpha/\pi)\lambda(\alpha,\zeta) \approx -1.33\alpha P_0/\pi$ is negative, which might be large and temperature dependent as well, whereas $N_F B_s(0) \approx -\frac{1}{4}\ln(\varepsilon_F/T)$ in this case. This means that, in some temperature regions, $|A_s| > |B_s(0)|$; therefore $F_0^a > 0$ and the Landau Fermi-liquid parameter in the spin channel in equation (47) becomes positive. Moreover $F_0^a(0)$ can even increase with decrease in temperature owing to the temperature dependence of P_0 in $\lambda(\alpha,\zeta)$. Thus, the spin susceptibility in equation (47) $\tilde{\chi}_s(0,0) \approx -N_F/[1+F_0^a(0)]$, in this case will decrease with decrease in temperature. Such temperature behaviour of $\tilde{\chi}_s(0,0)$ may have some relevance to the explanation of the spin-pseudo-gap behaviour in the underdoped region ($YBa_2Cu_3O_{7-x}$ and $La_{2-x}Sr_xCuO_4$) for cuprates [9, 33, 34] in the normal state. Furthermore, in this case, ($F_0^a(0) > 0$), according to the Landau Fermi-liquid theory; in the system there should exist a well defined undamped spin zero-sound mode. The dispersion relation for the spin zero-sound mode can be found from equation (45) for $\omega > v_F k$. From equation (56) in the strong-coupling limit ($\alpha \gg 1$) and with $\chi_0(k,\omega) = N_F[1/\sqrt{(1-v_F^2k^2/\omega^2)}-1]$ in equation (45) (the free-particle response function in the high-frequency limit, $\omega > v_F k$, for a 2D electron spectrum), the dispersion relation for the spin zero-sound mode turns into the form $\omega_s = v_s k$, where v_s is the spin-wave velocity and given by either $v_s = \sqrt{F_0^a/2}v_F \approx \sqrt{(\alpha|\lambda(\alpha,\zeta)|/2\pi)}v_F \approx \sqrt{(0.67\alpha P_0/\pi)}v_F$ for $F_0^a \gg 1$, or $v_s \approx v_F$ for $F_0^a \ll 1$. As seen, the velocity v_s of the zero-sound mode may depend on the interlayer spacing c because $\lambda(\alpha,\zeta)$ depends on it. The existence of the spin zero-sound mode in the case of strong coupling (whereas there is no sound mode in the charge channel in this case) seems to be in agreement with the Mermin [35] theorem which asserts that at least one of the modes ($m = 0$), zero sound or spin zero sound, must exist in the Fermi liquid at sufficiently low temperatures.

5. Conclusions

In summary, it is shown here that the vertex corrections for both the charge and the spin channels play an important role in the charge and spin responses of the Fermi liquid. It is also shown that the virtual pair (Cooper pair-like) excitations can contribute to both charge and spin responses of the Fermi liquid. This is in agreement with the MFL model proposed by Varma *et al*, to explain the universal anomalies in the normal state of cuprate high-T_c superconductors. In this sense the theory given here seems to be its microscopic origin.

The major approximations to derive equations (26) and (27) for the charge response and equations (47) and (48) for the spin response are based on several assumptions. First, it is assumed that the interaction has momentum and frequency extents of the order of the Fermi energy. Thus, as noted above, our consideration is suitable for non-retarded interactions such as Coulomb type, and cannot be used for retarded interactions such as the electron–phonon interaction when $\omega_{ph} \ll \varepsilon_F$ i.e. when the characteristic phonon frequency is much less than the Fermi energy. In the latter case the vertex corrections are not important, the Migdal [18] theorem applies and the adiabatic approximation is sufficient. Second, we assumed that N_F, the density of states, is a constant up to the Fermi energy. This means that our consideration is more suitable for the 2D energy spectrum where $N_F = m^*/\pi$.

The kernel of the two-particle interaction which appears in the equation for the three-point vertex part is evaluated in the first step of perturbation beyond the RPA. It includes three different contributions: the first-order screened exchange interaction, and two others representing, the interaction in the particle–hole channel, namely the direct screened and the Cooper-like second-order terms. The direct term corrects the first-order screened exchange, whereas the Cooper-like term represents the states that appear on addition or removal of two particles and has a logarithmic singularity with respect to the variable $\boldsymbol{p}' + \boldsymbol{p}$ as in the Cooper issue. The existence of such terms in the lowest order of perturbation was first indicated by Landau [37] in his theory of the Fermi liquid. The Cooper-like term is different from the well known Cooper exchange graph due to the identical initial and final momenta in scattering. This term appears in the perturbation series with a factor of 2 due to the spin summation and with a negative sign with respect to the conventional Cooper graph. We carried out the ladder summation of these three contributions to find the solution of the integral equation for the three-point vertex part. It is shown that the Cooper-like scattering produces the imaginary part of polarizability in the charge channel that contains the anomalous Fermi-liquid term $\sim -\omega/T$ in addition to the normal Fermi-liquid response $\sim -\omega/v_F k$. In other words the Cooper-like scattering induces the virtual pair excitations in addition to the usual single-particle excitations. In the spin channel the first step of perturbation leads to the first-order screened exchange interaction between particles only and thereby reproduces the spin response which is in an agreement with Landau's Fermi-liquid theory.

In addition, we have shown that our results can satisfactorily describe the deviation from the Korringa law that was observed in experimental studies of the nuclear-spin relaxation time in cuprates. Moreover, our results show the existence of an undamped spin-wave zero sound in the case of strong coupling. It seems that such a spin wave was observed in the neutron scattering studies of superconducting copper oxides in the normal state [36]. In addition, we have shown that the spin-psuedo-gap behaviour observed in the underdoped cuprates can also be explained in the framework of the correlated Fermi-liquid model. In this paper we do not make a detailed comparison of the present theory with the available experimental data for cuprates. Instead, we basically rely on the qualitative analysis performed by Varma and co-workers [10–12]. The detailed numerical calculations of both

the normal and the superconduction-state properties such as the dynamical conductivity $\sigma(\omega)$, etc, with the contribution of virtual pair excitations, which will make this paper too lengthy, are being undertaken and will be published in the future. As an example, we may evaluate the inverse quasi-particle lifetime $\tau_e^{-1}(\omega) = -2\,\mathrm{Im}\,\Sigma(p_F, \omega)$ (where $\Sigma(\boldsymbol{p}, \omega)$ is the single-particle self-energy) in combination with the irreducible response function in the charge channel given by equation (25). Our crude estimation of $\tau_e^{-1}(\omega)$ shows the present theory can satisfactorily describe, at least, the linear temperature dependence of resistivity in a wide temperature region, which was observed in most of cuprates in the normal state.

Acknowledgments

This work is supported in part by the US Air Force Office of Scientific Research under the grant AFOSR-91 0337 and the US Department of Energy under the grant DE-FG05-94ER25229.

References

[1] Gurvitch M and Fiory A T 1987 *Phys. Rev. Lett.* **59** 1337
[2] Batlogg B 1991 *Physica* B **169** 7
[3] For a review, see Iye Y 1992 *Physical Properties of High Temperature Superconductors III* ed D M Ginsberg (Singapore: World Scientific) p 302
[4] Kapitulnik A 1988 *Physica* C **153** 520
[5] Ong N P 1990 *Physical Properties of High Temperature Superconductors II* ed D M Ginsberg, p 463
[6] Tanner D B and Timusk T 1992 *Physical Properties of High Temperature Superconductors III* ed D M Ginsberg (Singapore: World Scientific) p 426
[7] Sugai S, Entomoto Y and Murakami T 1989 *Solid State Commun.* **72** 1193
[8] Cooper S L and Klien M V 1990 *Comments Condens. Matter Phys.* **15** 55
[9] Pennington C H and Slichter C P 1990 *Physical Properties of High Temperature Superconductors II* ed D M Ginsberg (Singapore: World Scientific) p 313
[10] Varma C M, Littlewood P B, Schmitt-Rink S, Abrahams E and Ruckenstein A E 1989 *Phys. Rev. Lett.* **63** 1996
[11] Littlewood P B and Varma C M 1992 *Phys. Rev.* B **46** 405
[12] Varma C M 1993 *J. Phys. Chem. Solids* **54** 1081
[13] Sire C, Varma C M, Ruckenstein A E and Giamarachi T 1994 *Phys. Rev. Lett.* **72** 2478
[14] Aslamazov L G and Larkin A I 1968 *Sov. Phys.–Solid State* **10** 875; 1968 *Phys. Lett.* **26A** 238; 1974 *Sov. Phys.–JETP* **40** 321
[15] Maki K 1968 *Prog. Theor. Phys.* **39** 897; 1973 *Phys. Rev. Lett.* **30** 648; 1974 *J. Low. Temp. Phys.* **14** 419
Thompson R S 1970 *Phys. Rev.* B **1** 327
[16] Ginzburg V L 1960 *Sov. Phys.–Solid State* **2** 1824
[17] Abrikosov A A, Gorkov L P and Dzyaloshinki I E 1964 *Method of Quantum Field Theory in Statistical Physics* (Englewood Cliffs, NJ: Prentice-Hall)
[18] Migdal A B 1958 *Sov. Phys.–JETP* **34** 996
[19] Nozieres P 1964 *Theory of Interacting Fermi System* (New York: Benjamin)
[20] Engelsberg S and Schrieffer J R 1963 *Phys. Rev.* **131** 993
[21] Mahan G D 1990 *Many Particle Physics* (New York: Plenum)
[22] Malozovsky Y M and Fan J D 1994 *Physica* C **231** 63
[23] Rice T M 1965 *Ann. Phys., Lpz.* **31** 100
[24] Virosztek A and Ruvalds J 1990 *Phys. Rev.* B **42** 4064
[25] Nozieres P and Pines D 1966 *The Theory of Quantum Liquids* (New York: Benjamin)
[26] Baym G and Pethick C 1991 *Landau Fermi-Liquid Theory* (New York: Wiley)
[27] Fetter A 1974 *Ann. Phys., NY* **88** 1
[28] Malozovsky Y M, Bose S M, Longe P and Fan J D 1993, *Phys. Rev.* B **48** 10 504
[29] Pines D 1955 *Solid State Physics* vol 1, ed H Erenreich, F Zeitz and D Turnbull (New York: Academic)
[30] Berk N F and Schrieffer J R 1966 *Phys. Rev. Lett.* **17** 433
[31] Imai T, Shimizu T, Yasuoka H, Ueda Y and Kosuge K 1989 *J. Phys. Soc. Japan* **57** 2280

[32] Malozovsky Y M and Fan J D 1994 *Phys. Rev.* B **49** 4334
[33] Slichter C P 1996 *Strongly Correlated Electronic Materials* ed K S Bedell *et al* (New York: Addison-Wesley) at press
[34] Monthoux P and Pines D 1994 *Phys. Rev.* B **50** 16 015
[35] Mermin N D 1967 *Phys. Rev.* **159** 161
[36] Birgeneau R J and Shirane G 1989 *Physical Properties of High Temperature Superconductors I* ed D M Ginsberg (Singapore: World Scientific) p 188
[37] Landau L D 1959 *Sov. Phys.–JETP* **35** 70